JGR Planets

RESEARCH ARTICLE
10.1029/2021JE007126

Special Section:
The Curiosity rover's investigation of Glen Torridon and the surrounding area

Active Ground Patterns Near Mars' Equator in the Glen Torridon Region of Gale Crater

Bernard Hallet[1], Ronald S. Sletten[1], Michael Malin[2], Nicolas Mangold[3], Robert J. Sullivan[4], Alberto G. Fairén[4,5], Germán Martínez[6,7], Mariah Baker[8], Juergen Schieber[9], Javier Martin-Torres[10,11], and Maria-Paz Zorzano[5]

[1]Department of Earth and Space Sciences, University of Washington, Seattle, WA, USA, [2]Malin Space Science Systems, Inc., San Diego, CA, USA, [3]Laboratoire de Planétologie et Géodynamique, UMR6112 CNRS, Faculté des Sciences, Université de Nantes, Nantes, France, [4]Cornell Center for Astrophysics and Planetary Science, Cornell University, Ithaca, NY, USA, [5]Centro de Astrobiología (CSIC-INTA), Madrid, Spain, [6]Lunar and Planetary Institute, Houston, TX, USA, [7]Department of Climate and Space Sciences and Engineering, University of Michigan, Ann Arbor, MI, USA, [8]Center for Earth and Planetary Studies, National Air and Space Museum, Smithsonian Institution, Washington, DC, USA, [9]Department of Geological Sciences, Indiana University, Bloomington, IN, USA, [10]Department of Planetary Sciences, University of Aberdeen, Aberdeen, UK, [11]Instituto Andaluz de Ciencias de la Tierra (UGR-CSIC), Granada, Spain

Abstract On Mars, near the equator, much of the terrain in Gale Crater consists of bedrock outcrops separated by relatively smooth, uniform regolith surfaces. In scattered sites, however, distinct patterns—in the form and texture of the ground surface—contrast sharply with the typical terrain and with eolian bedforms. This paper focuses on these diverse, intriguing ground patterns. They include ∼1 to >10 m-long linear disruptions of uniform regolith surfaces, alignments, and other arrangements of similar-sized rock fragments and shallow, ∼0.1 m-wide sandy troughs 1–10 m in length. Similar features were recognized early in the Mars Science Laboratory (MSL) mission, but they received only limited attention until Curiosity, the MSL rover, encountered striking examples in the Glen Torridon region. Herein, the ground patterns are illustrated with rover images. Potential mechanisms are briefly discussed in the context of the bedrock composition and atmospheric conditions documented by Curiosity. The evidence suggests that the patterns are active forms of spontaneous granular organization. It leads to the hypothesis that the patterns arise and develop from miniscule, inferred cyclic expansion and contraction of the bedrock and regolith, likely driven by oscillating transfers of energy and moisture between the atmosphere and the terrain. The hypothesis has significant implications for studies of contemporary processes on Mars on both sides of the atmosphere-lithosphere interface. The ground patterns, as well as ripples and dunes formed by the wind, constitute remarkable extra-terrestrial examples of granular self-organization, complex phenomena well known in diverse systems on Earth.

Plain Language Summary Gale crater, which is near Mars' equator (4.5°S latitude), is generally rocky with sand and rocks scattered between extensive bedrock exposures. However, in a few local sites, distinct natural patterns mark the ground with ∼0.1 m-wide, sand-lined troughs and rocks arranged geometrically. We use detailed images from Curiosity, the Mars Science Laboratory rover, to illustrate these intriguing patterns in the Glen Torridon area, where they are widespread. We suggest they are currently active in the dry rock debris at the surface and driven by the sustained shrink-swell activity of the underlying bedrock. This inferred activity, which likely results from variations in moisture and temperature in the lower Mars atmosphere, could generate these ground patterns, much like vibrations or analogous cyclic disturbances cause patterns to form naturally in diverse settings with granular materials of different sizes and shapes. The inferred cyclic shrink-swell behavior of the shallow subsurface and underlying transfers of energy and mass may be of broad interest because of their potential implications for studies of processes shaping the Mars landscape and occurring in the lower atmosphere. These ground features, as well as ripples and dunes formed by the wind, are visible examples of extra-terrestrial self-organization.

Key Points:

- Near Mars' equator, sandy troughs and organized rock fragments locally form distinct patterns suggestive of active ground deformation
- Unlike patterned ground on Earth, the ground patterns in Gale Crater form in thin, dry regolith overlying jointed bedrock
- Atmosphere-surface exchange of energy and water vapor is inferred to drive self-organization through cyclic subsurface volume changes

Supporting Information:

Supporting Information may be found in the online version of this article.

Correspondence to:

B. Hallet and R. S. Sletten,
hallet@uw.edu;
sletten@uw.edu

Citation:

Hallet, B., Sletten, R. S., Malin, M., Mangold, N., Sullivan, R. J., Fairén, A. G., et al. (2022). Active ground patterns near Mars' equator in the Glen Torridon region of Gale Crater. *Journal of Geophysical Research: Planets*, *127*, e2021JE007126. https://doi.org/10.1029/2021JE007126

Received 9 NOV 2021
Accepted 31 MAY 2022

Author Contributions:

Conceptualization: Bernard Hallet, Ronald S. Sletten
Funding acquisition: Michael Malin
Investigation: Bernard Hallet

1. Introduction—What Are These Ground Patterns?

This paper illustrates and characterizes the diverse ground patterns encountered in Glen Torridon (GT), the focus area of this special issue of the Journal (Bennett et al., 2022). The patterns range from 1 to 10 m-long, 0.1 m-wide sand-lined troughs (sand bands) bordering bedrock to distinct domains with clear geometric organization in

Writing – original draft: Bernard Hallet, Ronald S. Sletten, Robert J. Sullivan, Juergen Schieber, Javier Martin-Torres
Writing – review & editing: Bernard Hallet, Ronald S. Sletten, Michael Malin, Nicolas Mangold, Robert J. Sullivan, Alberto G. Fairén, Germán Martínez, Mariah Baker, Juergen Schieber, Javier Martin-Torres, Maria-Paz Zorzano

terms of size, shape, orientation, and/or alignment of mineral and rock fragments. The self-portrait of Curiosity (Figure 1) displays, in the foreground, a common type of ground pattern: curving bands of sand between bedrock exposures at one of the sites of special interest. The patterns are rare yet widespread, occurring locally at scattered sites. They are small (typical width of 1 m or less) and contrast with the relatively smooth and texturally uniform, dusty surface of loose sand and scattered pebbles usually present between bedrock exposures (Figure 2). They also differ clearly from rover tracks and from characteristic eolian sand ripples and dunes, which are discussed by Sullivan et al. (2022).

The ground patterns are intriguing because they are enigmatic. Why do they form? What are they trying to tell us about the conditions and processes under the surface? Unlike sand ripples and dunes that clearly reflect sediment transport by wind, the formative processes for these patterns are less obvious; we suggest that they result from minuscule, recurrent volume variations of the bedrock driven by environmental fluctuations at the surface. Although these subsurface volume variations have not been observed directly, probably because they are small and out of sight under a regolith cover, they can be inferred with confidence based on considerable evidence for significant surface-atmosphere vapor exchange and studies documenting volume changes in diverse rocks under laboratory conditions. We suggest that these volume variations are active in Gale Crater and over much of the planet's surface, driven by surface-atmosphere exchange of energy and water vapor, with broad implications for atmosphere-surface interactions and the evolution of the Mars surface.

We begin with a brief review of previous work on ground patterns on Mars and then illustrate examples of exceptionally well-developed and clearly illustrated patterns scattered across GT, a shallow 0.4 km-wide valley on the flanks of Mount Sharp. The patterns are particularly distinct in the phyllosilicate-rich region in the valley's lowest ∼1.4 km-long reach (Figure 3). This descriptive section is followed by a short introduction to the inferred underlying processes, the pertinent material properties, and the environmental data. The observations and data are presented, and their implications are discussed. Another publication will report on similar ground patterns recognized throughout the Mars Science Laboratory (MSL) mission and compare them with patterned ground on Earth; it will also explore potential formative processes.

2. Background

The first observations of ground features on Mars date back to the earliest landers. Mutch et al. (1977) highlighted distinct shallow sand-lined troughs at the Viking Lander 2 site in the mid-latitudes (48°N). They illustrated troughs reaching ∼10 m in length and local relief of 0.1–0.4 m. They noted the contrast between the troughs and the relatively smooth landing sites, which were chosen before landing "for safety reasons, for their topographic blandness." They also considered several formative mechanisms and settings: (a) contraction fractures forming in cooling lava to form contraction fractures, (b) fractures forming in desiccating water-saturated clay-rich regolith minerals, and (c) thermal expansion and contraction of frozen ground. They favored the third mechanism, discussing the observations in the context of previous work on polygonal patterned ground in terrestrial permafrost and concluding that "The total appearance of a terrestrial sand-filled crack closely resembles that of the feature observed on Mars."

Subsequent satellite observations have revealed ubiquitous polygonal patterned ground across middle to high latitudes (∼30°–80°) on Mars (e.g., Kostama et al., 2006; Kuzmin, 2005; Levy et al., 2009; Mangold, 2005). In addition, lander-based images and considerable theoretical work have focused on the polygonal networks among the "Periglacial landforms at the Phoenix landing site" at 68°N where ground ice was suspected before landing and confirmed by Phoenix (Mellon et al., 2008, 2009). Ground patterns and dry regolith features that are very similar to those addressed herein were also observed by Horne (2018) close to the Martian equator (2°S) between 2004 and 2017 with the Mars Exploration Rover (MER) Opportunity in the Meridiani Planum region. He states: "evidence of additional (to eolian bedform formation and cratering) and hitherto-unrecognized surface processes is offered by two types of geologically young, small-scale features imaged by Opportunity: (a) leveed fissures and (b) gutters." Horne (2018) infers that these features could signify recent transient liquid and gas emissions.

Here we focus on ground patterns and features characteristic of the GT area in Gale Crater. They also seem "geologically young" or active and are comparable with those imaged by Opportunity; they differ significantly, however, as they lack the leveed fissures and signatures of liquid and gas emissions suggested by Horne (2018). They are also quite distinct from those reported elsewhere on Mars and Earth. They lack the geometric regularity

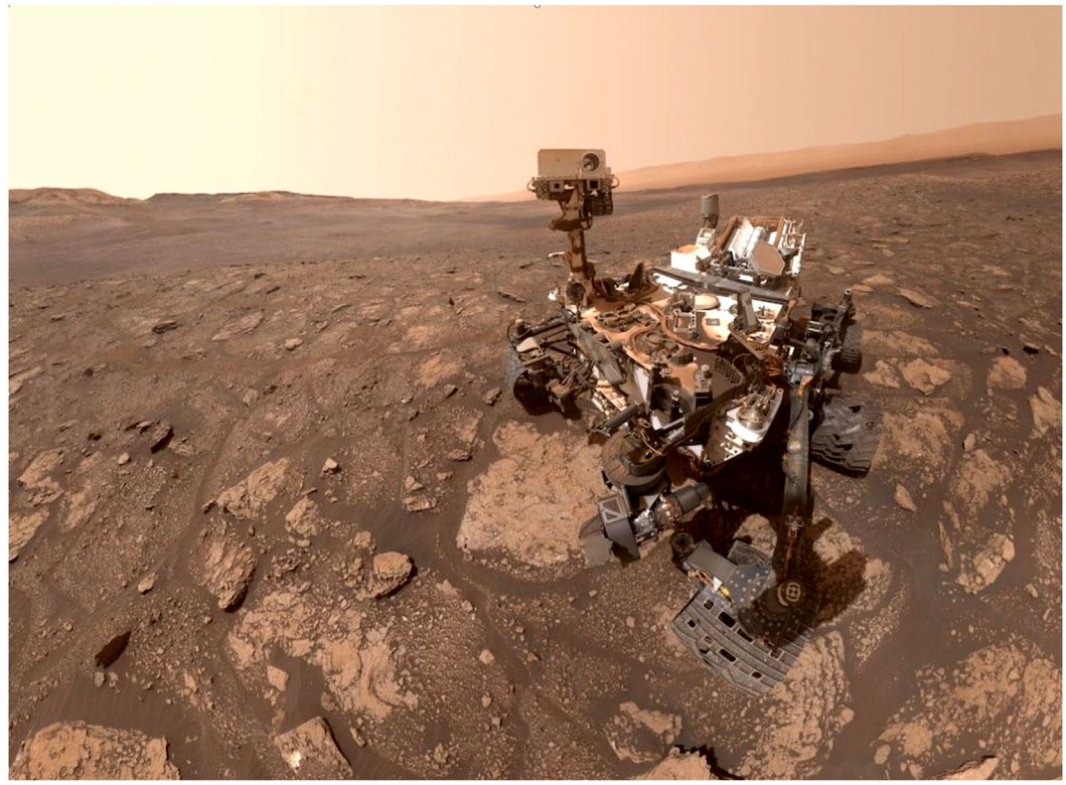

Figure 1. The Mars Science Laboratory rover, Curiosity, seems puzzled by the sand bands weaving between bedrock blocks on the ground surface. Self-portrait at the Mary Anning study site in Glen Torridon, a broad valley near the Mars equator. Composite of images from the Mars Hand Lens Imager acquired on sol 2922 and released by NASA on 12 November 2020 (https://www.jpl.nasa.gov/news/nasas-curiosity-takes-selfie-with-mary-anning-on-the-red-planet).

and distinct polygonal networks typical of many middle- to high-latitude areas on Mars and periglacial permafrost regions on Earth. Unlike polygonal patterned ground on Earth, which is best developed in thick, laterally uniform, permanently frozen alluvium and other unlithified material (permafrost), GT ground patterns generally occur close or adjacent to bedrock exposures; they do not occur far from exposed bedrock. The GT patterns also differ from others in scale. With typical lateral dimensions and relief on the order of 0.5 and 0.02 m, respectively, they are smaller than those reported from high latitudes on Mars (Mellon et al., 2009; Mutch et al., 1977) and Earth. Lastly, the patterns appear to be active despite the current absence of liquid water and ice, as addressed in the discussion section.

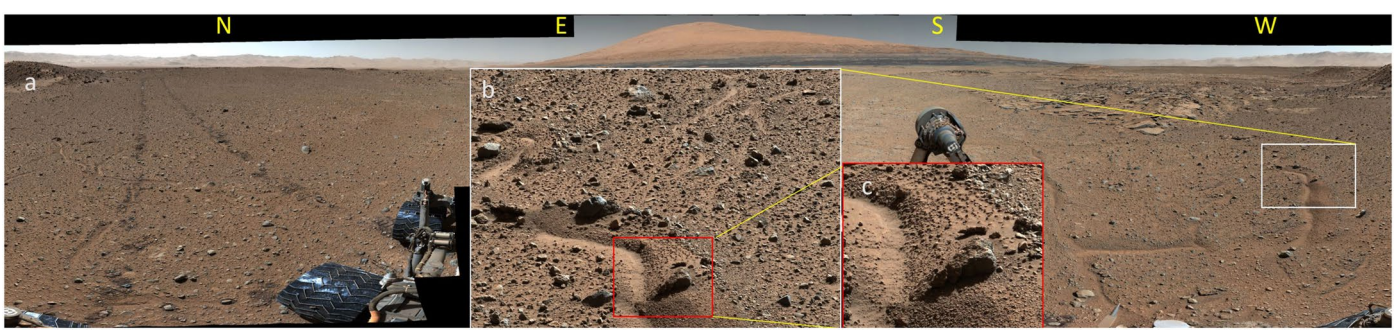

Figure 2. (a) 360° Mastcam panorama, centered on Mount Sharp, illustrates ground patterns and their setting (Sol 592, ML-002492). Cardinal directions are labeled along upper edge of image (yellow capital letters). A few isolated sandy troughs to the W-SW and surface scuffs to the N stand out in the exceptionally flat terrain and relatively smooth pebbly surface. Rover tracks to the N provide a useful scale; they are 2 m apart. (b) shows the local relief and textural difference between the sand in the trough and the pebbly regolith (Sol 590, MR-002481). (c) highlights a portion of the trough that features spaced-out granules of uniform size. A higher resolution version of the insets is provided in Figure S1.

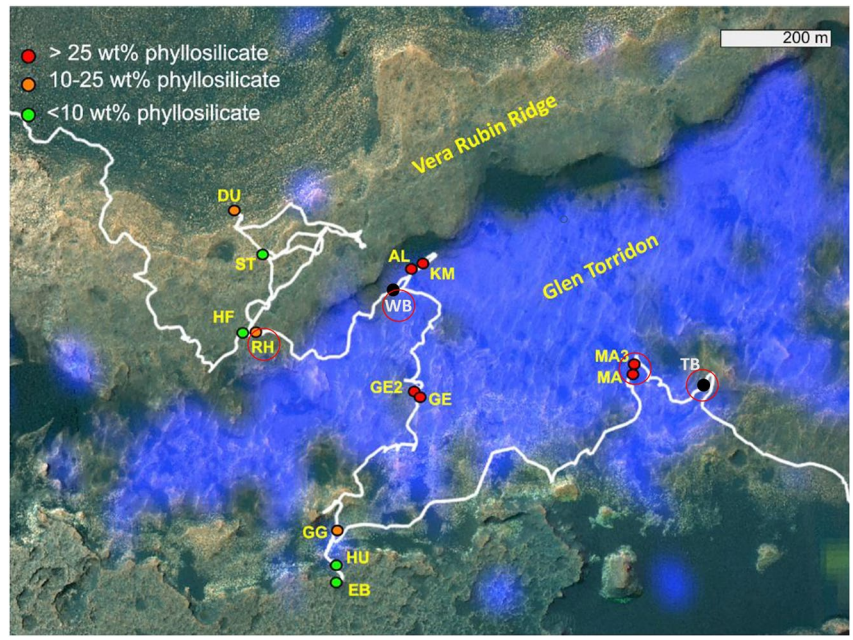

Figure 3. Compact Reconnaissance Imaging Spectrometer for Mars map of Fe/Mg-smectite spectral absorption detections from orbit in the Glen Torridon region, with the darkest blue representing the deepest spectral absorptions attributed to clay minerals (a.k.a. phyllosilicates), and from drill holes analyzed by CheMin (Chemistry and Mineralogy instrument), which revealed smectite abundances represented by colored dots. Black dots were added to indicate the location of two additional sites with informal acronyms WB and TB for Woodland Bay and The Benches. Acronyms for the other ground pattern sites of special interest are RH for Rock Hall and MA for Mary Anning. Large red open circles highlight the location of features discussed in the text. Map and caption adapted from Figure 5 of Tu et al. (2021). Map courtesy of Valerie Fox.

This paper complements and supplements Horne's (2018) paper; it presents new, detailed rover-based images of small-scale ground features that differ from eolian bedforms on Mars, and it improves the constraints on their ages. The images are accompanied by diverse data on the substrate composition and the environmental conditions. The strong, MSL mission-wide interest in the GT region enabled exceptional documentation of distinct ground patterns that were particularly instructive for two reasons. First, the features are unusually well developed, and the observations were more detailed and covered longer periods than in other areas in Gale Crater. Second, the more extended observations yielded image sequences suggestive of significant ongoing surface change and pattern activity.

We suggest that the active ground patterns have broad implications for diverse geomorphic processes on Mars. Our work adds to a set of studies of a present-day active atmosphere-regolith water cycle (e.g., Bishop et al., 2021; Chevrier & Rivera-Valentin, 2014; Martín-Torres et al., 2015; Schmidt et al., 2017; Vakkada Ramachandran et al., 2021; Wang et al., 2019). Collectively, this research suggests that the surface of Mars is currently being shaped by environmentally driven volumetric changes of the near-surface bedrock, as well as eolian, impact, insolation, and gravitational processes.

3. Data and Methods

The primary data utilized in this work are images acquired on the Martian surface by the MSL rover's Mastcam stereo imaging system (Bell et al., 2017; Malin et al., 2017). This system consists of two cameras with different focal lengths (Left, 34 mm, and Right, 100 mm) mounted side-by-side on the rover's Remote-Sensing Mast, about 2 m above the ground surface. They are referred to as M34 and M100, or ML and MR, respectively. Malin et al. (2017) provide detailed information on the camera, and associated hardware and software, used to produce the color images. Labels for images and mosaics generally start with ML or MR and include the observation's sequence number; for instance, "ML_mcam12220" designates a left-eye, 34 mm focal length camera mosaic produced from the Mastcam sequence "mcam12220" (in this example, a mosaic of 3 by 2 frames was acquired on sol, or Martian day, 2293 of the MSL mission). This work also utilizes image data from the arm-mounted Mars

Hand Lens Imager (Edgett et al., 2012), which provides close-range, hand lens-quality images when placed near ground targets and wide-angle rover self-portrait mosaics from an elevated arm position (e.g., Figure 1).

Mastcam stereo mosaics were acquired at key sites, allowing three-dimensional, mm-scale modeling of these surfaces. Digital elevation models (DEMs) were derived using several programs developed by the Malin Space Science Systems (MSSS) software group and the Ames Research Center's (ARC) Machine Vision Group. Stereo pair images with the Left image (M34) and the Right image (M100) were first decompressed, converted back to a 16-bit representation of the intrinsic 12-bit data, radiometrically calibrated, Bayer color filter array interpolated (de-mosaiced), and geometrically corrected for camera lens distortion. Using the ARC-MSSS DEM photogrammetric software, the image pairs were processed to create Triangulated Integrated Networks (TINs—3D meshes) in OpenInventor (.iv) format with texture (color) from the higher resolution image (M100). Multiple adjacent meshes were combined into a VRML .wrl file (Virtual Reality Modeling Language), which could be viewed and measured in Antares, a visualization program with many capabilities, including reading VRML files and their components, and displaying these directly as textured meshes. These meshes were converted to DEMs using TIN2DEM, which creates a 32-bit DEM and an orthographic projection of the texture (8 or 24 bit), elevation, and orthoimage files. These files were then run in the ARC Desktop Exploration of Remote Terrain (DERT) software to create resolution pyramids of the data (Layerfactory) and then read into the DERT viewing and measurement program, which includes many measurement capabilities. The profiles in the paper were all generated using DEMs and orthoimages. The horizontal scale of the texture is based on the M100 pixel scale. The vertical scale is based on interpolation between the M34 and M100 scales, including the separation of the cameras and the emission angle of the images. The vertical resolution varies over the DEM from a few tenths of a millimeter to about 1 mm. Because each DEM is computed by digitally combining two images that differ in scale, the lower resolution camera generally dictates the horizontal scale of the DEM. The process that creates the DEM interpolatively resamples the topographic data to the texture scale, which comes from the M100, but the topographic data are inherently at the resolution of the M34 images.

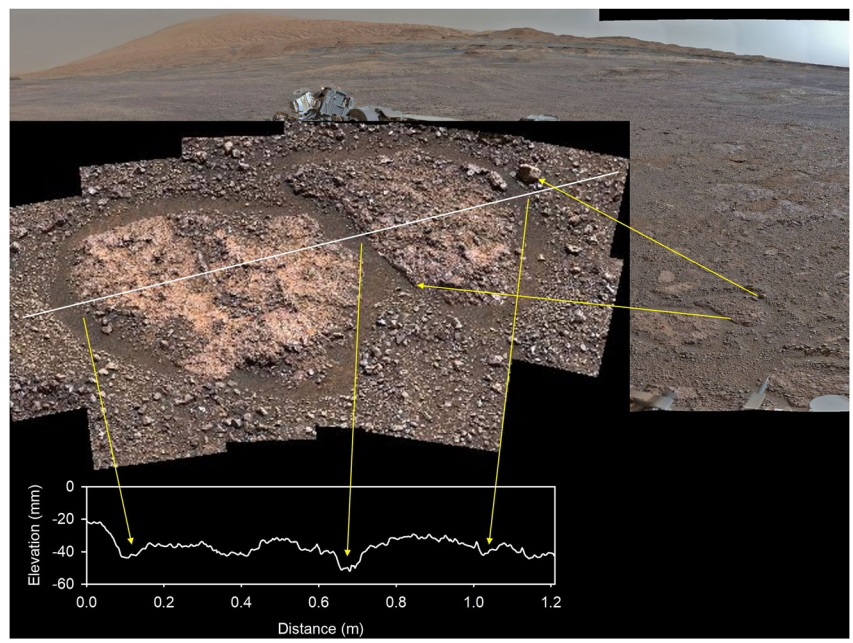

Figure 4. Panorama dominated by Mt. Sharp (background image) was acquired on Sol 2264 (ML-012114) near the top of Vera Rubin Ridge before entering the clay-rich Glen Torridon region. Center inset. Double circle pattern at Rock Hall (Sol 2259, MR-012091) consists of bedrock blocks bordered by a 0.1 m-wide sand-filled trough. The elevation profile defines the ~20 mm micro-relief and ~0.5 m diameter of the blocks; note the ~5-fold vertical exaggeration.

4. Observations

4.1. Ground Patterns in Glen Torridon

In this section, we illustrate ground patterns that are exceptionally well developed and/or that occur where Curiosity remained longer than usual to detect surface changes and to acquire detailed images, as well as numerous analyses and measurements conducted by other MSL teams. A few examples were selected, mainly from four GT sites: Rock Hall, Woodland Bay, Mary Anning, and the Benches. The last site stands out from the others in lacking extensive imaging and analyses, but it illustrates exceptionally well the close connection between ground patterns and the jointed bedrock.

4.1.1. Rock Hall

Upon entering GT, uniform bands of sand on the ground between and adjacent to bedrock outcrops were so distinct relative to the surouding rocky ground surface that they elicited attention from the entire MSL science team for the first time in the mission. For much of the team, they seemed to signal novel features and phenomena; they were intriguing in themselves as well as for their potential geologic and atmospheric significance. The shallow troughs partially filled with wind-blown sand framing two adjacent bedrock exposures at the Rock Hall site were striking visually (Figure 4). Comparable features have been seen on Mars, starting with the Viking landers (Figure 10 in Mutch et al., 1976), but those were highly asymmetrical "horseshoe-shaped depressions interpreted as scour marks on the windward side of blunt blocks." They contrast with the sand bands at Rock Hall that form a uniform border around each bedrock block lacking directionality, which could suggest wind erosion.

4.1.2. Woodland Bay

This area displayed one of the most distinctive ground patterns in the GT region (Figure 5). It is defined by linear troughs in thin regolith that turn abruptly, presumably following an underlying orthogonal set of bedrock joints. Small-scale surface characteristics of the patterns warrant special attention, as they figure extensively in the text below; they are defined and illustrated in Figures 5 and 6, which display distinct linear regolith features: (a) broad sandy troughs (0.1–0.2 m wide, ∼1 m long, and ∼30 mm deep) that are common at all study sites, (b) trenches that are sharp-edged surface depressions tens of millimeters in width and ∼1 m in length along the axis of many broad sandy troughs, and (c) one shallow, narrow ∼4 mm-wide and 0.15 m-long depression that formed within a 61-sol period in a sandy trough as documented by Mastcam images (Figures 6c and 15b). Distinct textural domains comprised of well-sorted clasts of different sizes are typical of the troughs. In particular, trough sides are commonly covered or consist of granules that are unusually uniform in size, shape, and spacing and distinctly smaller than rock fragments that line the crest of the trough sides (Figure 5; Sol 2424 inset).

4.1.3. Mary Anning, Upper Ollach (90+ Sols)

An exceptional sequence of Mastcam images of a sandy trough, informally named Upper Ollach, at Mary Anning documented considerable grain motion not only during the drilling but long after the drilling stopped. The post-drilling motion is of general interest because it documents progressive slope evolution and grain displacements that may help understand similar natural processes likely to occur universally on comparable surfaces in Mars' equatorial regions.

The distinct axial trench in Upper Ollach received attention as soon as it was imaged due to its steep sides that apparently truncate sand ripples (Figures 7 and 8). Its fresh appearance was surprising because the ongoing sand transport and ripple migration would tend to readily fill in the trench, smooth the sand surface, and heal the ripple truncations. Interest in this trough and its axial trench developed further as additional imagery and results of eolian process studies became available and showed wind transport of sand to be unusually active at Mary Anning (Sullivan et al., 2022).

Figure 9 illustrates the short-term surface response to drilling disturbances at Upper Ollach. Supporting Information (Text S1 and animated GIF, Figure S4) documents the response over a period of 56 sols. First, vibrations from drilling caused subsidence and local surface collapse along the center of the axial trench (Figure 9, sol 2840 inset), which undermined its sides and formed trough-parallel scarps and fissures as the sand on the steep sides shifted downslope. Second, downslope sand motion and eolian transport of sand naturally converged on the lowest areas, partially infilling the center of the trench. More detailed analyses of the surface displacements in response to the drilling and the evolving microtopography are underway but are beyond the scope of this paper.

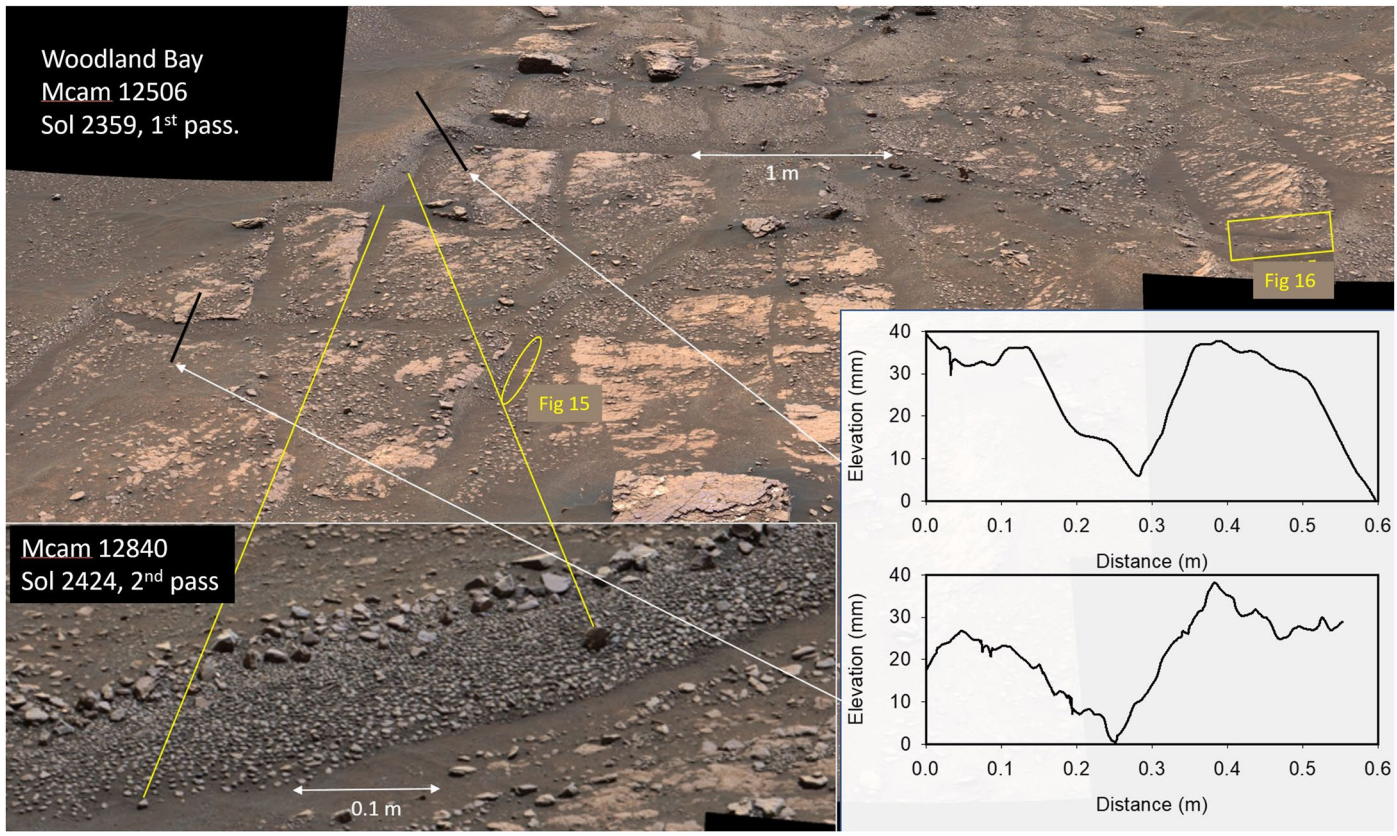

Figure 5. Overview of an orthogonal trough network in thin regolith over jointed bedrock in Woodland Bay (Sol 2359, ML-012506; lower half is also shown Figure 6a). Yellow lines help locate the subscene (portion of Sol 2424, MR-012840) that shows the clear sorting according to size and shape. It also displays the uniform spacing of subrounded clasts along trough sides below a crest lined with larger, pebble-sized angular rock fragments. The short black lines show the location of elevation profiles (note the ~5-fold vertical exaggeration), which start at the lower end of the black lines. The yellow ellipse corresponds to those in Figure 15, and the yellow rectangle outlines the field of view in Figure 16. A higher resolution version of the subscene and bordering areas is provided in Figure S2.

The vibrations from percussion drilling were, of course, a major artificial driver, but we suggest in the discussion (see Section 5.9) that the response of the regolith to the disturbance provides valuable clues about natural surface processes.

4.1.4. The Benches

This panorama of the area known informally as The Benches (Figure 10a) is made up of 122 individual Mastcam ML images taken on sols 2946 and 2947 (https://www.jpl.nasa.gov/images/curiositys-view-of-benches-on-mars). It displays clear examples of sandy troughs extending beyond joints in the exposed bedrock (Figures 10b and 10d). Fractured rock blocks are common at the margins of bedrock exposures; they tend to be steeply inclined and aligned with the edge of the sorted regolith along major bedrock joints (Figure 10c).

4.2. Ground Patterns in Gale Crater Beyond Glen Torridon

Many ground patterns were seen throughout the mission before reaching, and after traversing, GT (e.g., Figure 2). Figure 11 illustrates a distinct example encountered in a different geologic terrain, far from GT; the pattern is highlighted by bands of rock fragments that are parallel to the irregular, orthogonal perimeter of outcrops of the Murray formation (Mount Sharp Group) near the transition from Sutton Island to Blunts Point members (Fedo et al., 2022). Many rock fragments are steeply tilted, in contrast with the nearly horizontal bedding of the bedrock. The white oval in Figure 11b highlights a near-vertical, light-colored rock splinter that probably originated from a patch of light-colored vein filling on a bedding plane, similar to those in the center foreground of Figure 11.

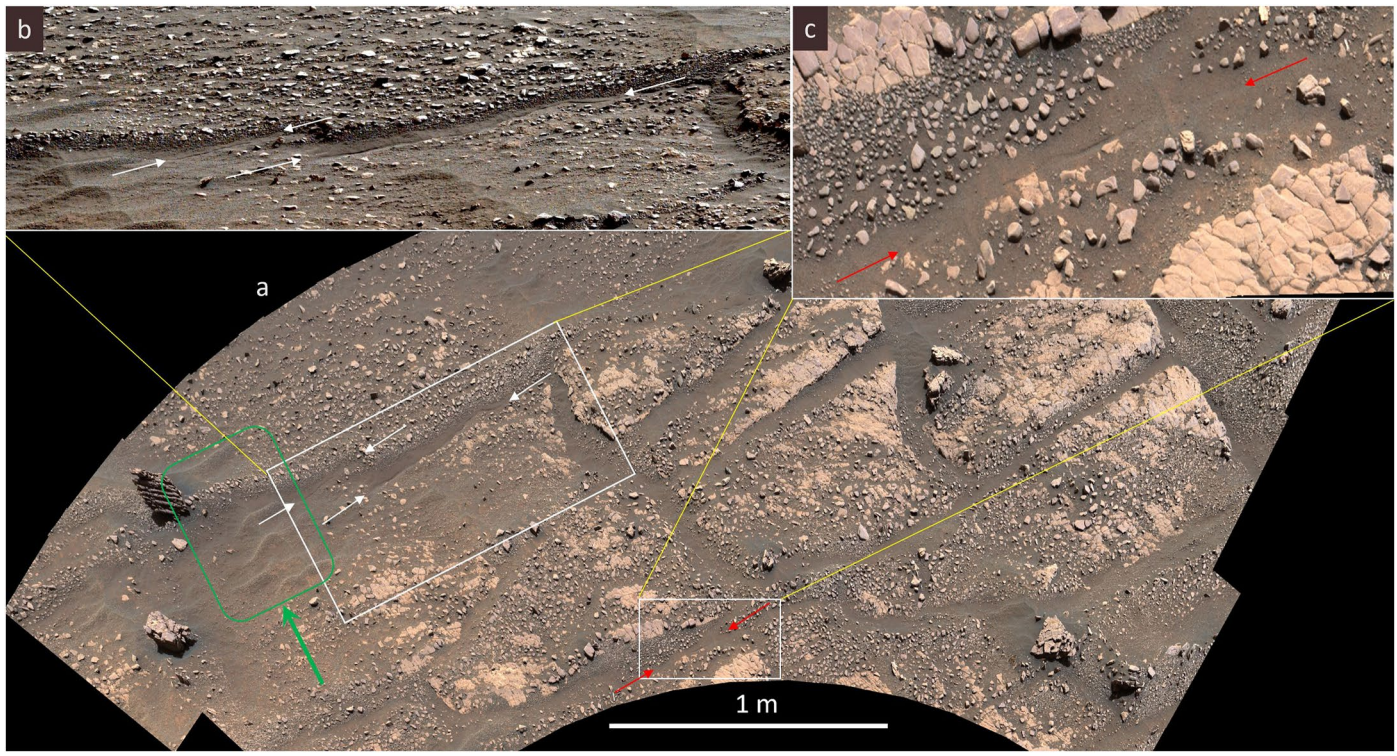

Figure 6. Morphological characteristics of ground patterns: (a) meter-long and ~0.2 m-wide sandy troughs between bedrock blocks are bordered by 30 mm-high ridges littered with rock fragments in Woodland Bay (Sol 2427, MR-012853; area also shown in Figure 5). This vertical, ortho-rectified image locates the subscenes (outlined in white) and ripples of coarse wind-blown sand (green rectangle); green arrow shows the approximate direction of the most recent sediment transporting winds. Panel (b) shows the textures and topographic details of the site (Sol 2422, ML-012835). White arrows in both panels (a and b) point to distinct sharp-edged, ~50 mm-wide, and ~1 m-long trenches along the axis of sandy troughs. (c) Narrow, linear depression formed between sols 2359 and 2420 (also see Figure 15b). Red arrows point to subtle apparent extensions of the depression.

4.3. Organization of Rock Fragments on Regolith Surfaces

In addition to the well-sorted domains and tilted rock fragments in the regolith between bedrock exposures, the location and orientation of fragments are commonly far from random. Figure 12 shows large rock fragments clustered along major through-going bedrock structures, probably joints. In contrast, similar-sized fragments are rare away from the major structures. Moreover, nearly all large rock fragments in the scene are at the edges of regolith bands (Figure 12, insets a and b). In addition, Figure 13 illustrates a network of sand-filled troughs between bedrock outcrops, commonly with large rock fragments along their perimeters. A closer examination reveals that many smaller fragments are aligned with one another along trough margins (see insets).

4.4. Bedrock Composition and Environmental Data

Most of the ground patterns discussed here occur in smectite-rich terrain, as is evident from Figure 3, the (Compact Reconnaissance Imaging Spectrometer for Mars) map of Fe/Mg-smectite spectral absorption detections from the orbit, which are consistent with analyses of borehole tailings (Thorpe et al., 2021; Tu et al., 2021). Little mineralogy data exist for the regolith, but it is not expected to differ substantially from typical bedrock. Generally, ground patterns are not limited, however, to the GT region or to smectite-rich terrain. For instance, at Rock Hall, the underlying bedrock is not smectite-rich.

Much is known about the modern near-surface Martian climate from the Curiosity rover's REMS (Rover Environmental Monitoring Station) ground temperature and air humidity sensors (e.g., Martínez et al., 2021), which are directly pertinent for ground patterns. Figure 14 illustrates the seasonal and other variations in ground surface temperature and near-surface (1.6 m) relative humidity (RH) during the first ~3456 sols of the mission. For graphical clarity, the large diurnal fluctuations are not shown.

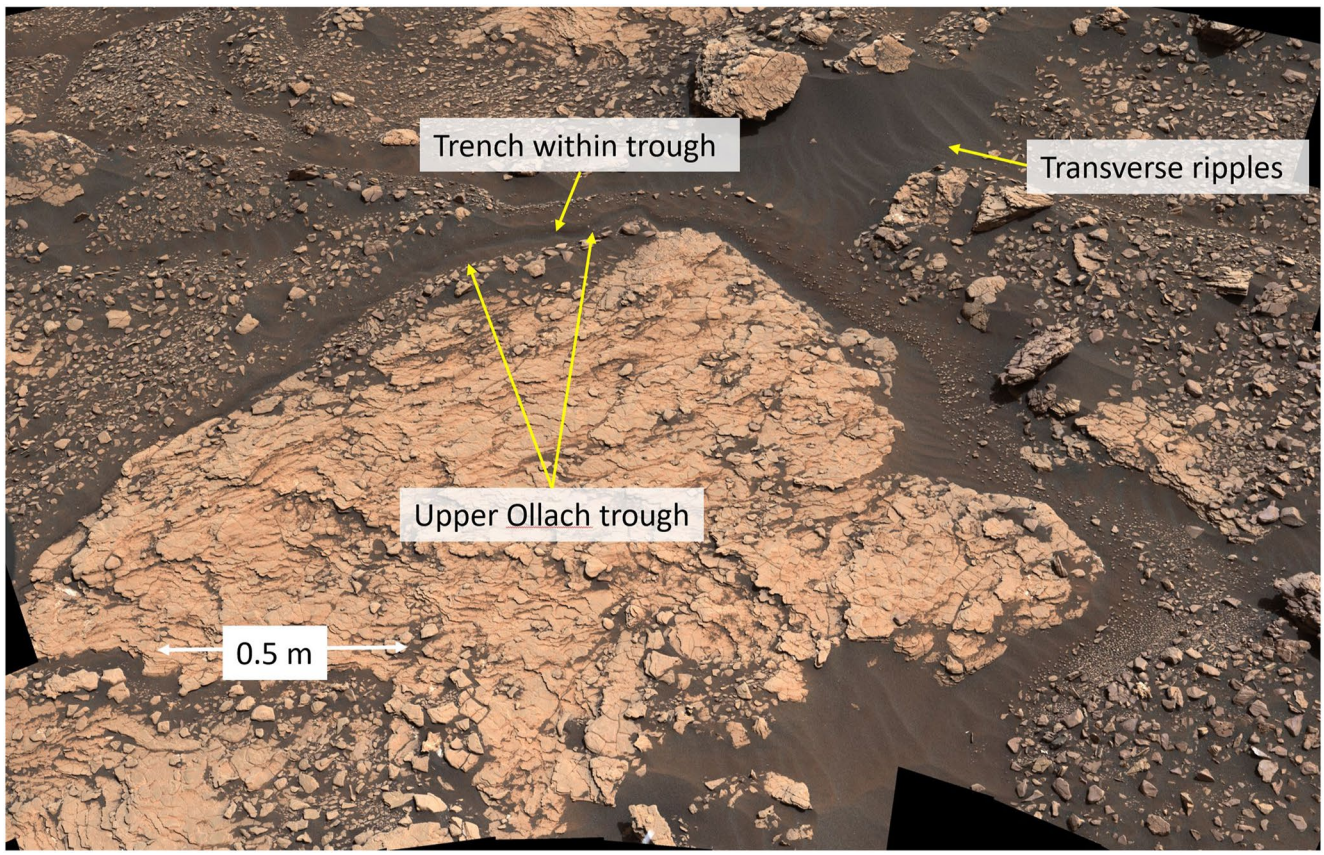

Figure 7. Upper Ollach, a sandy trough bordering bedrock at Mary Anning, was extensively studied because of clues that it was active. A key clue is the distinct, steep-sided trench within the trough; it is absent in nearby troughs where transverse sand ripples (indicated in upper right) show no hint of disruption along the trough, as discussed in the text (Sol 2833, MR-014822).

5. Interpretation and Discussion

5.1. Actively Forming Ground Patterns

We use the adverb, actively, in the subtitle for the patterns discussed here to distinguish them from their potential static counterparts formed in the geologic past. Active is a relative term, however, dependent on the timescale of interest. Two timescales, tens of days and decades, pertain to the ground patterns in GT. The shorter timescale is based on changes observed in Mastcam images acquired on sols 2359 and 2420. These observations document the distinct, ~0.2 m-long and ~4 mm-wide, linear depression that developed within a ~61 sol period in a relatively broad (~0.2 m-wide) sandy trough at Woodland Bay (Figures 6c and 15b). It is noteworthy that rover disturbances were relatively small at this site and restricted to the immediate vicinity of the rover wheels, and there was no drilling activity. Moreover, Curiosity remained in this vicinity for only a few sols and did not rove over the site. Aside from nearby tracks left by the rover wheels, Curiosity left no impact visible in Mastcams on or near this pattern.

The decadal timescale derives from the common occurrence of distinct sharp-edged axial trenches indicating they are evidently not getting filled in significantly or effaced by impacts of blowing sand even where eolian sand transport is active. Hence, these trenches must be actively widening and/or deepening at least as fast as or faster than they trap wind-blown sand. Without this activity, the trenches would smooth and disappear from the terrain on a timescale that can be readily estimated. The timescale for wind-blown sand to fill a depression depends on its size and the sand flux, which can be estimated from the depression size and the migration rate of nearby eolian ripples. As wind-driven saltating grains impact ripple surfaces, they splash and move sand grains along the surface. The collective motion of these splashed grains (the "reptation flux") results in overall ripple

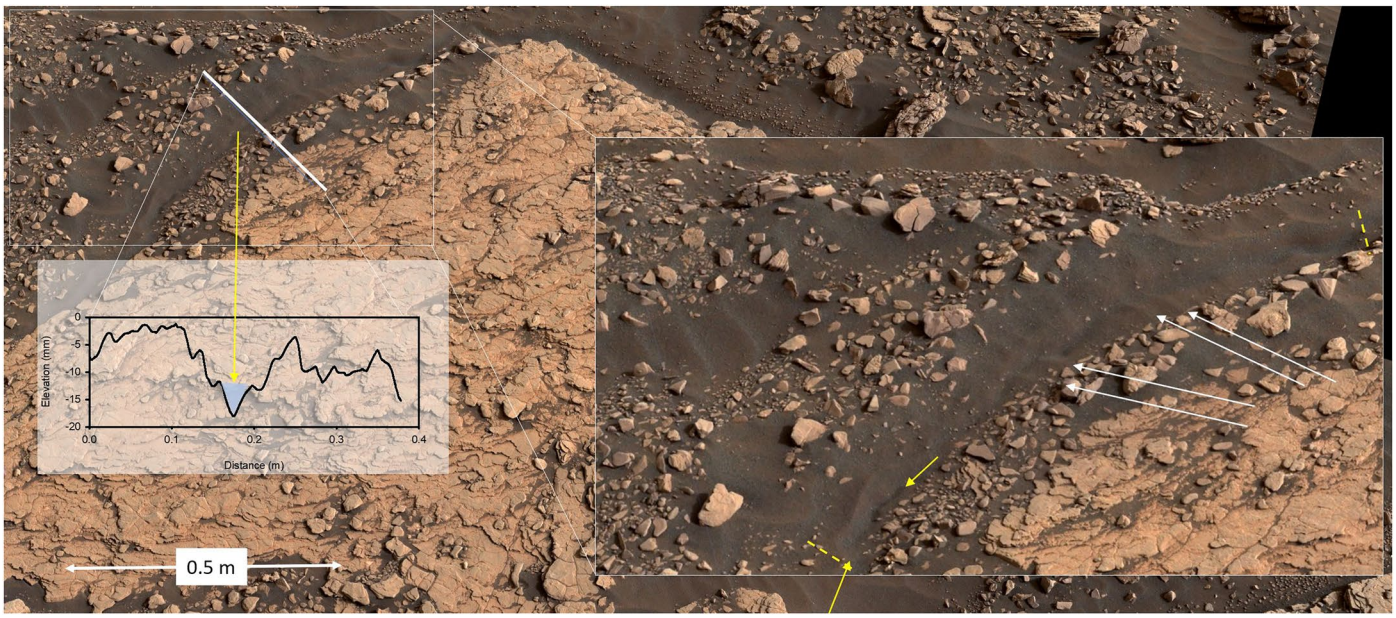

Figure 8. The Upper Ollach trough at Mary Anning in its original condition, 9 days before the first drilling at this site. The steep-sided trench along the trough axis (highlighted by blue shading in the elevation profile; note ~6-fold vertical exaggeration) suggests recent subsidence in the center of the trough and apparent truncation of sand ripples at the edges of the trench. In the closer view in the inset on right side, white arrows point to truncated ripples, yellow arrows highlight a section of the trench that appears partially open to the atmosphere, and the short yellow dashed lines delimit the lateral boundaries of the fields of view in Figure 9 (Sol 2829, ML-014816).

migration. For example, the observed ripple crest migration over 45 sols during the windy season at the Mary Anning drill site (sols 2859–2904) implies a reptation flux, per unit distance transverse to the transport direction, of $\sim 2 \times 10^{-6}$ m^2 sol^{-1} (Sullivan et al., 2022), which is lower than the flux estimates at the Bagnold Dunes visited earlier in Curiosity's traverse (Baker, Lapotre, et al., 2018). Approximating the cross-section of the axial trench at Upper Ollach as a triangle, 30 mm wide and 5 mm deep, based on the elevation profile (Figure 8), its cross-sectional area is $\sim 10^{-4}$ m^2. A trench of this size that is transverse to the ripple migration direction and traps all reptating grains would fill in only ~50 sols. This timescale may not be surprising given the distinct expression of the trench edges and fragile features of the sandy surface (Figure 16) that would be readily effaced by the impacts of saltating grains in a terrain with much wind-driven sand transport.

This trench would likely fill more slowly, however, for several reasons. The reptation flux value applies only to the windy season in the MSL operating area (Baker, Lapotre, et al., 2018; Baker, Newman, et al., 2018; Bridges et al., 2007; Newman et al., 2017), and the trench would unlikely be perpendicular to the direction of ripple migration. Hence, an order of magnitude lower sand flux is likely more realistic for estimating the timescale for filling the trench, raising it to ~500 sols. Increasing this timescale another order of magnitude, approaching a decade, would account roughly for the irregular spatial distribution of small, active ripple patches in GT relative to trench locations. Many trenches are not currently in the downwind path of actively migrating ripples, so they are unlikely to be filled soon despite the current sand mobility observed in GT. Although this decadal estimate is simplistic and not well constrained, it constitutes perhaps the first quantitative index of the age for regolith features that appear active on the Mars surface and that developed long before Curiosity's arrival.

For such depressions to survive longer than decades, the net input of wind-blown sand would have to be offset by active regolith processes that function as sand sinks or enlarge the depression during this period. For instance, sand could filter below the ground surface along cracks or voids in the regolith and underlying bedrock, or the depression could enlarge by widening and deepening. Both of these processes have been documented in analog systems on Earth, the sand-wedge polygonal patterned ground, as described in the next section. Lastly, we note that the timescale of decades for the age of surface details that appear fresh is broadly consistent with Horne's (2018) descriptive wording: young, small-scale surface features, and it improves the constraints on the meaning of "young" in this context by three orders of magnitude.

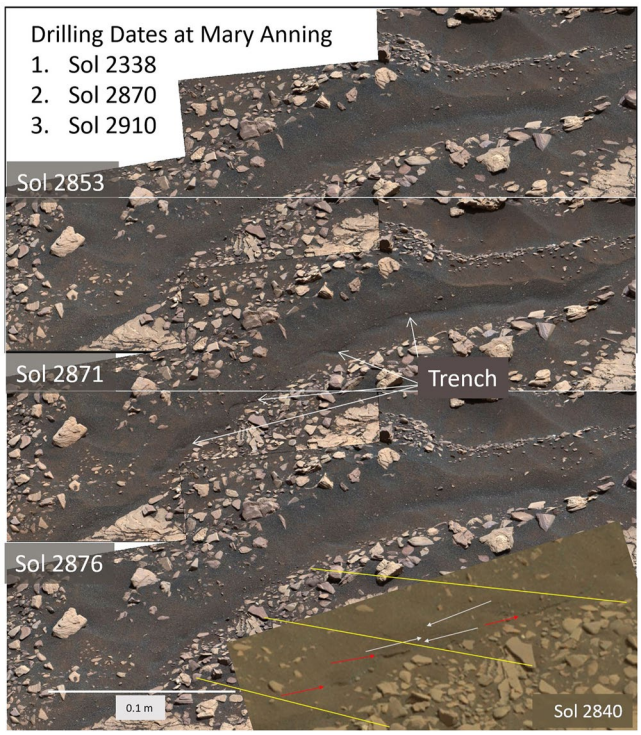

Figure 9. Upper Ollach trough evolution starting on Sol 2853, after 15 days of recovery from the significant impact of vibrations (shown in Sol 2840 inset, lower margin; arrows point to new scarps [white] and collapsed areas [red] from drilling the first hole at Mary Anning on Sol 2838). The sol 2871 image was acquired the day after drilling the second hole. The drilling evidently triggered subsidence along the trough's center, deepened the axial trench, and steepened the sandy slopes, causing loose sand and granules to quickly fill the trench bottom. It reveals new subsidence and suggests local sand filtering into preexisting subsurface voids along the trench axis (shown by long arrows). Five sols later, on Sol 2876, the trench had healed considerably, as evident from the distinct smoothing of the top edges of the trench. A higher resolution version of the Sol 2871 mosaic (Figure S3) and an animated GIF (Figure S4) are provided in the Supporting Information.

Vastly longer timescales than decades also have relevance for the observed granular organization and ground patterns to develop fully. Constraining the longest timescales from geomorphic evidence is challenging, however, because uncertainties increase with time due to many factors, including the significant changes in the topography and climate that are likely during the much longer periods. In particular, large environmental changes are expected on theoretical grounds for periods of 1–10 Myr and longer due, to orbital change. Notably, according to Laskar et al. (2004), "It is remarkable that the present value of the obliquity of Mars (~25.19°) is very far from its mean value, evaluated over 4 Gyr (~37.62°) …This suggests that the present dry and cold Martian climate is probably not representative of the past current environmental conditions." Madeleine et al. (2009) examined numerically the global-scale environmental consequences of various obliquity histories for a range of surface conditions, including dustiness, surface albedo, and thermal inertia. They report numerous relevant results, among which their Figure 12a is particularly interesting; it shows GCM-computed net ice accumulation rates in equatorial regions reaching and exceeding 1 mm yr^{-1} at, or near, Gale Crater using a Mars obliquity of 35°, a common value in the past, beyond 5 Myr. It supports the notion that Gale Crater experienced major environmental changes and was possibly mantled with ice in the late Amazonian, as recently as 5 Myr ago.

More recently, Mellon and Sizemore (2022) used numerical simulations to study ground-ice stability in the past 2.5 Myr in the shallow subsurface at all landing sites on Mars. Whereas ground ice is currently unstable except for polar regions, they suggest that ground ice "would have been stable at all the landing sites for extended periods of tens of Kyr when the obliquity exceeded about 29°–33°. The most recent such episode would have occurred about 500 Kyr ago." They conclude with a statement of direct relevance to ground patterns: "The periodic occurrence of shallow ice for 20–50 Kyr may facilitate the formation of periglacial landforms such as polygonal ground and sorted rocks >500 Kyr ago in equatorial regions." Indeed, shallow ice would help account for relict polygonal patterned ground in Gale Crater near Curiosity's landing site (Oehler et al., 2016) and may have helped form the ground patterns in GT. Moreover, Mitrofanov et al. (2022) reported evidence for unusually high hydrogen abundances in the central part of Valles Marineris, which suggests that considerable residual subsurface ice may currently exist within a meter of the surface near the equator on Mars even at low altitude.

5.2. Formative Processes: Insights From a Terrestrial Analog

Little is known about the formative processes of equatorial ground patterns on Mars but studies of similar features on Earth provide valuable insights. Still, one needs to be mindful of using these insights in studies of Mars phenomena because of the dearth of relevant subsurface data from Mars and the considerable differences in surface environments and properties of materials on the two planets.

The ground patterns in Gale Crater share distinct similarities with certain forms of patterned ground in periglacial areas on Earth. Among the diversity of terrestrial patterned ground, the sand-wedge polygons of the Dry Valleys in Antarctica constitute, perhaps, the closest analog that has received significant research attention (Black, 1973; Hallet et al., 2011; Mutch et al., 1977; Pewe, 1959; Sletten et al., 2003). For instance, Figure 17a illustrates a distinct, compound trough that is remarkably similar, in form, size, and surface texture, to a trough outlining sand-wedge polygons in Antarctica (Figure 17b). Moreover, these polygons can serve as particularly instructive analogs because they are relatively well understood. They form much like ice-wedge polygons that were elucidated by a seminal study of the underlying processes in a terrestrial context (e.g., Lachenbruch, 1962); it provided a sound foundation for theoretical work, a half-a-century later, on the patterned ground at high latitudes on Mars (e.g., Mellon et al., 2008, 2009).

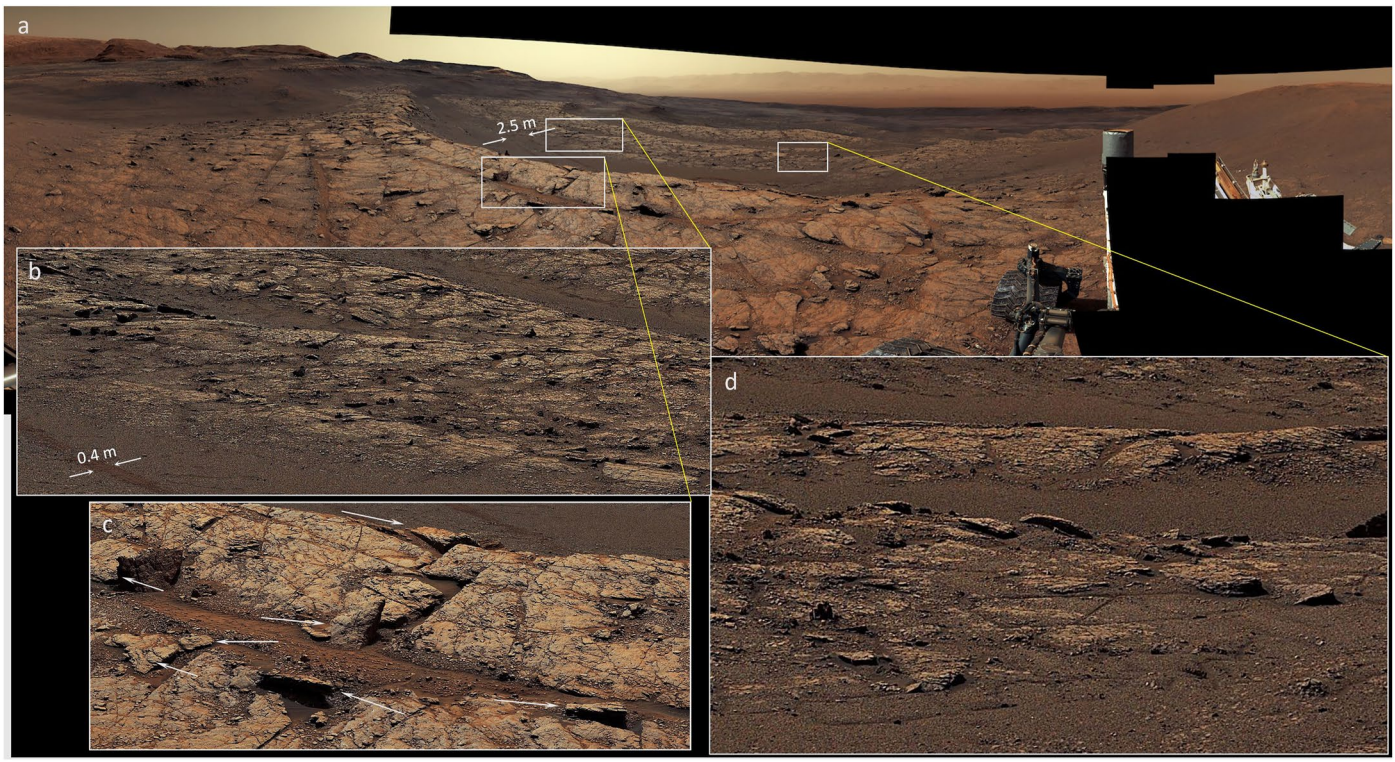

Figure 10. (a) Overview of The Benches, an area showing long bands of loose rock debris, probably covering near-vertical bedrock joints (Sol 2946, ML-015374, panels (a and c)). (b and d) Linear disruptions of the uniform regolith surface within 1–2 m of bedrock outcrops. (c) Fractured rock blocks (white arrows), common at the margins of exposed bedrock, tend to be tilted steeply (upended) and roughly aligned with the edge of the regolith (Sol 2947, MR-015378).

Sand-wedge polygons are widespread in the Dry Valleys of Antarctica. In these and other arid, cold regions, thermal contraction cracks form and open at the ground surface during cooling periods and partially fill with wind-blown sand and other fine-grained debris. This sand infilling, which contrasts with the ice wedges typical of moist permafrost areas, prevents the cracks from closing fully during warming periods. The cracks reopen during subsequent cooling periods, permitting additional sand infilling, thereby incrementally growing a wedge of sand. With time, the ground surface on either side of the crack is deformed and raised by the growing sand wedge to form a characteristic pair of symmetrical ridges separated by a trough with an axial trench over the crack (Hallet et al., 2011; Pewe, 1959). The progressive growth of sand-wedges has been examined by monitoring the distance between steel rods driven into the frozen regolith across contraction cracks (Figure 17b). Sequential distance measurements between paired rods reveal a progressive annual divergence averaging up to ~1 mm across sand-wedges in the Dry Valleys (Berg & Black, 1966; Sletten et al., 2003).

In contrast with polygonal patterned ground on Earth, which is best developed in thick frozen sediments away from exposed bedrock, the ground surface in GT on Mars is rarely marked by troughs or cracks away from bedrock exposures, suggesting that tensile stresses seldom develop in the dry regolith, or reach magnitudes sufficient to fracture the regolith. At least two factors could account for this observation: (a) the cohesion of the regolith may be insufficient to transmit stresses over distances much larger than the size of regolith particles and approach the meter-scale of the ground patterns in GT, and (b) volumetric changes in the underlying bedrock may be too small or too slow to generate significant tensile stresses in the regolith before they relax. The tendency for troughs to border bedrock exposure in GT has not been observed on Earth, as far as we know; we presume that they are not evident on Earth because relatively active terrestrial surface processes fill small depressions readily. In GT, troughs in the dry regolith may form only near the bedrock where the regolith is so thin that (a) it does not preclude significant volumetric cycling in the underlying bedrock by damping environmental variations, and (b) the regolith surface is directly influenced by the underlying bedrock; it simply subsides as fine-grained regolith particles filter into bedrock voids.

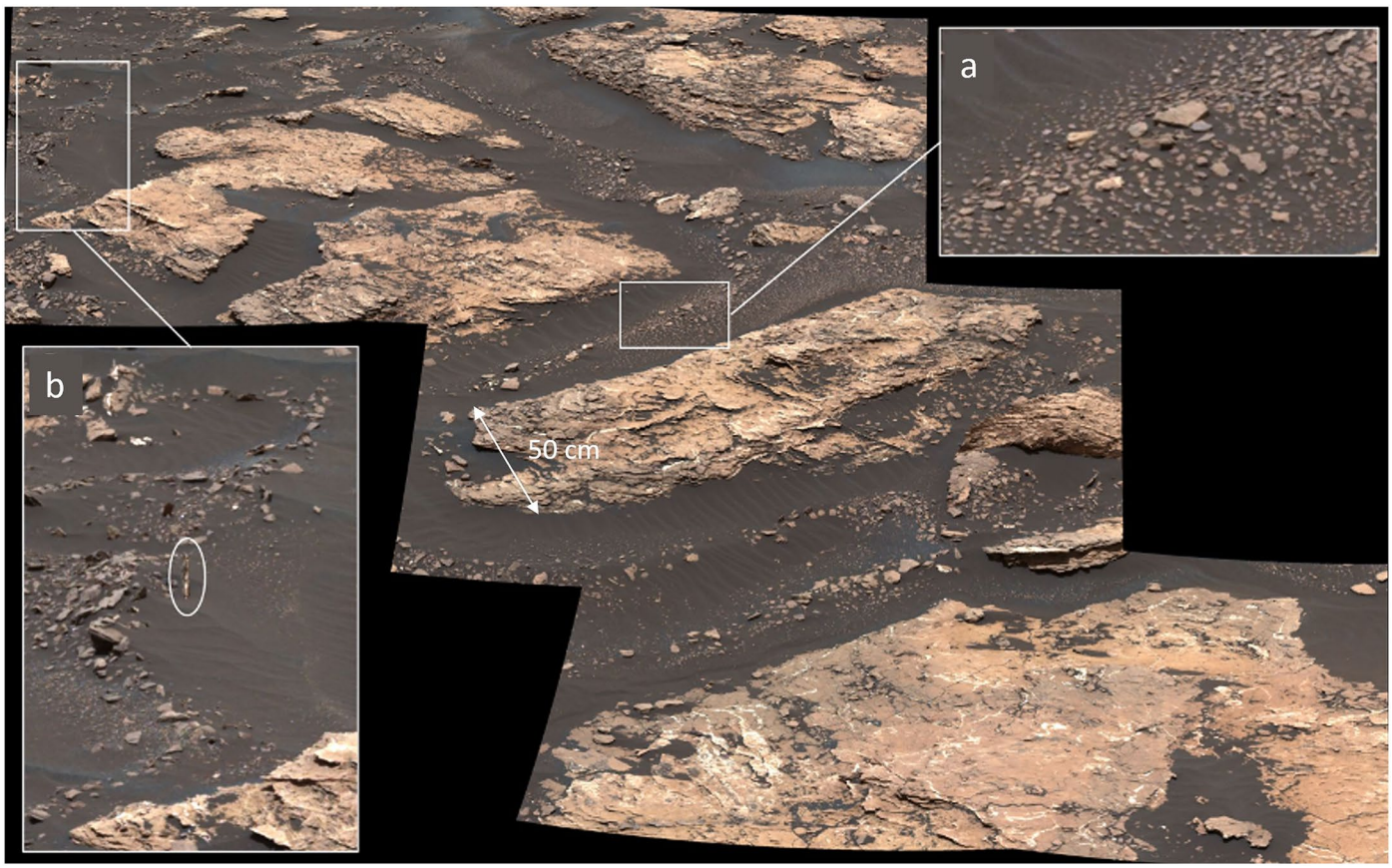

Figure 11. Mid-mission example of a ground pattern dominated by stone lines in sorted regolith between bedrock exposures (Sol 1677, ML-008702). Insets highlight significant details: (a) clasts are well-sorted and organized spatially according to size, the larger ones concentrating along low ridges. Note the relatively uniform clast spacing. (b) Series of relatively large, angular clasts form low ridges that weave between the outcrops. The white oval highlights a near-vertical splinter of light-colored rock (probably a mineralized vein).

Terrestrial sand-wedge patterned ground is an attractive analog for active ground patterns in the equatorial regions of Mars, except that there is little, if any, contemporary bulk water or ice near the surface. On Earth, ice is a central ingredient in the large volumetric oscillations that cause widespread polygonal patterned ground in permafrost terrain, and water figures centrally in the formation of sorted patterns—circles and stripes—in alpine and polar regions. Lacking these key ingredients in Gale Crater, we propose an alternate hypothesis for pattern formation and activity in dry regolith.

5.3. Hypothesis for Sorting and Pattern Formation in Dry Regolith

We infer that bedrock and overlying regolith undergo small cyclic volumetric changes near the ground surface, driven by exchanges of energy and moisture with the atmosphere and modulated by fluctuations in atmospheric conditions. Further, we hypothesize that these cyclic volumetric changes drive the organization of rock fragments, the formation and infilling of voids in the subsurface, and the development of patterns in the dry regolith.

According to this hypothesis, the pattern development in regolith has much in common with the equivalent behavior in diverse systems in which granular media is driven by vibrations or other recurrent mechanical forcings. The size segregation and pattern formation manifested in these "driven" granular systems caused by almost any difference in particle properties—particle size, shape, or density—have been the subject of extensive research summarized in recent books: for example, Granular Patterns (Aranson & Tsimring, 2008) and Segregation in Vibrated Granular Systems (Rosato & Windows-Yule, 2020). This research provides a rich context for the hypothesis, and ongoing research continues to advance understanding of the phenomena. For instance, Gajjar et al. (2021) studied the size segregation of irregular vibrated granular materials by tracking particle motion continuously.

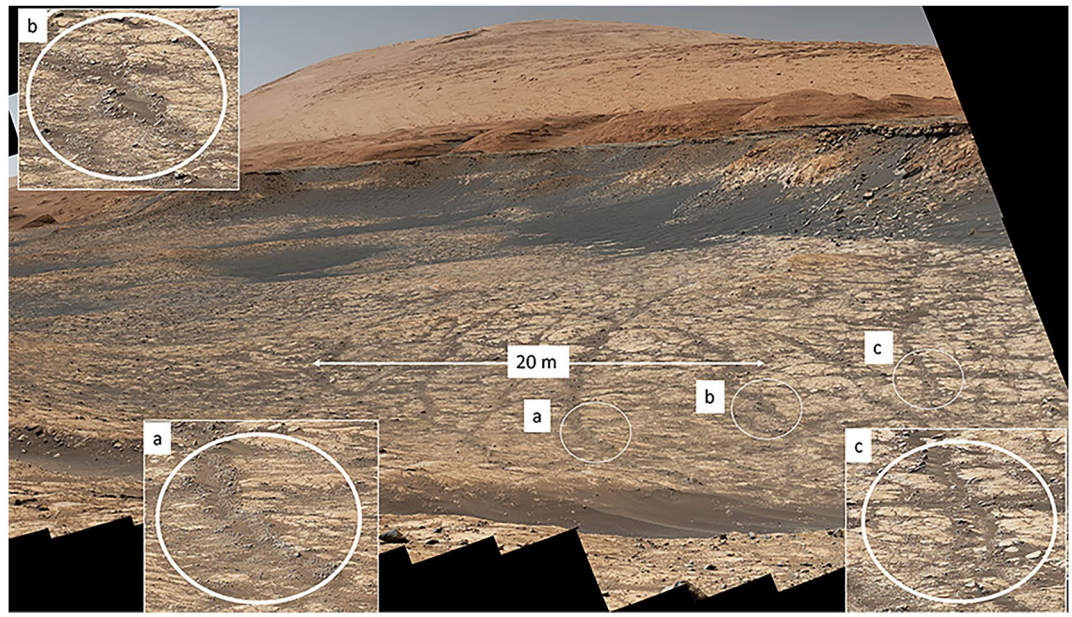

Figure 12. Panorama of eastern Glen Torridon (Sol 2641, MR-013727) shows an extensive bedrock exposure, perhaps a bedding plane with abundant, angular rock fragments along long, continuous bedrock structures, probably major joints. Large rock fragments seem to gather, or form at the margins, and less commonly along the axis, of regolith bands. Insets (a and b) poorly sorted fragments form discontinuous ridges that border wide regolith bands. (c) Angular fragments trace a line of varying width along the axis of a regolith band.

In contrast with previous work, their study focuses on the role of particle shape and orientation in sorting and vertical migration (kinetic sieving). Their findings that larger particles tend to rise and rotate toward the vertical have direct implications for the organization of debris on dry planetary surfaces, including the surface of Mars. For instance, the bedrock blocks in GT shown in Figures 10 and 12 may have become aligned and rotated toward the vertical, and the thin lithic fragment in Figure 11 may have been tilted steeply and aligned with the nearby bedrock surface by the cyclic expansion-contraction and associated granular processes that drive the formation of ground patterns. Again, caution is in order, however, in making these inferences when using insights guided by laboratory experiments with granular material subjected to energetic external excitation in the radically different context of slow, non-inertial, cyclic volumetric changes in regolith on Mars. Major differences are expected

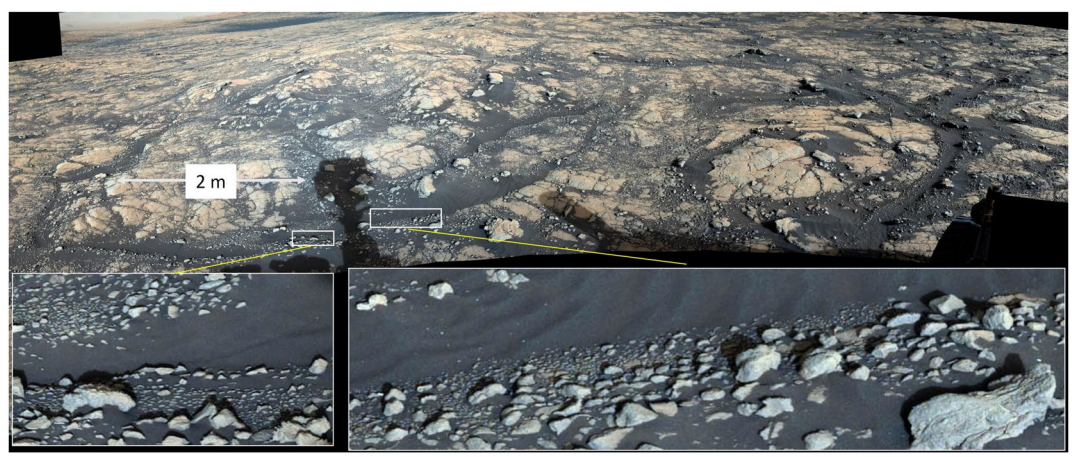

Figure 13. Extensive network of sandy troughs bordered by relatively large rock fragments between bedrock outcrops (Sol 2745, ML-014396). Insets show the distinct alignment along trough margins and preferred solid orientation of smaller clasts parallel to the margins.

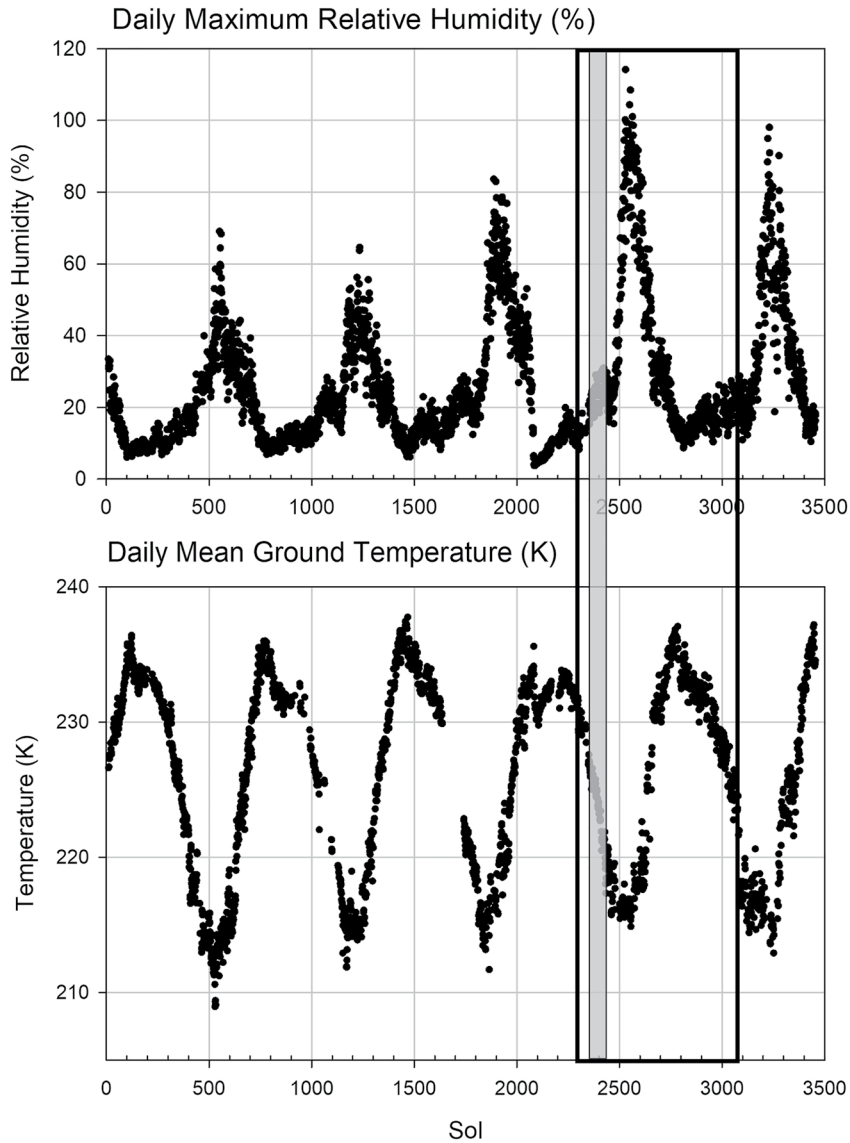

Figure 14. Curiosity rover's Rover Environmental Monitoring Station environmental measurements on Mars for the entire Mars Science Laboratory (MSL) mission up to April 2022, MSL sol 3456. Upper time series: daily maximum relative humidity at 1.6 m; lower series: daily mean ground surface temperature. The box marks the time interval of the Glen Torridon traverse, and the shaded area highlights when the rover passed by Woodland Bay.

between the behavior of granular material in these experiments and in regolith on Mars, but important similarities between these systems are also likely to be robust and instructive.

In addition to the expansion-contraction activity, wind likely contributes to the organization of rock fragments on the ground surface. Wind is clearly responsible for striking sand patterns and landforms: dunes, ripples, and drifts. It has also long been known that wind can sort small rock fragments and move larger rocks by eroding and redepositing the underlying sand (e.g., Bagnold, 1941). Motivated in large part by images "of the Mars Exploration Rover Spirit landing site (that) exhibit a nonrandom (i.e., uniformly spaced) distribution," Pelletier et al. (2009) explored the process further. Using wind tunnel experiments and numerical models, they examined the evolution of mixed grain size eolian surfaces with a distribution of clasts; it tends to become more uniform through time. The sandy surfaces in Gale Crater with scattered granules and pebbles are often unusually uniform in size and spacing (e.g., Figure 2c, Figure S1, and sol 2424 inset in Figure 5), a distribution atypical of patterned ground on Earth; they probably owe their origin primarily to self-organizing eolian processes.

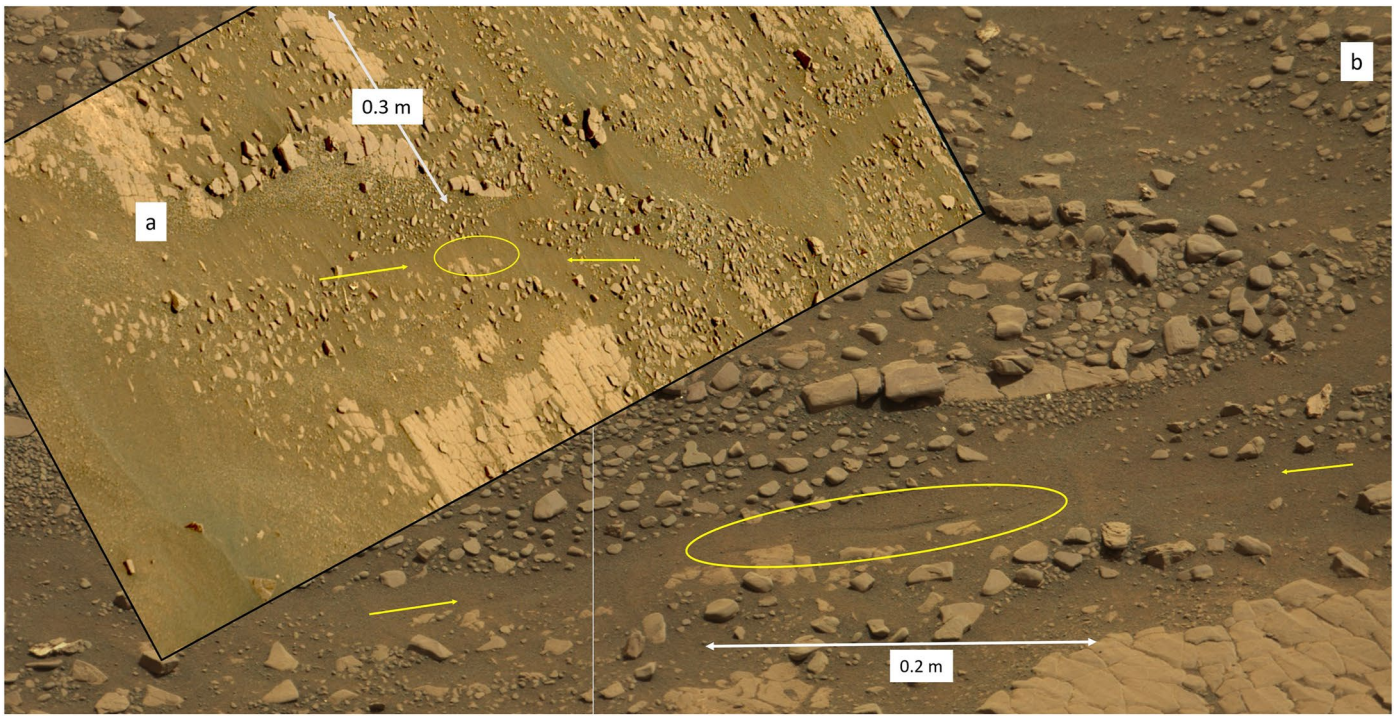

Figure 15. Documentation of a narrow, linear depression at Woodland Bay developed between sols 2359 and 2420. (a) Initially, a shallow trough lined with sand and rock fragments showed no surface disruption (Sol 2359, ML-012506). (b) A narrow linear depression developed within the following 61 sols before the site was first re-imaged on sol 2420; it appears to have been stable in the subsequent 7 sols (Sol 2427, MR-012853). A similar view is shown in Figure 6c. In both panels (a and b), the yellow ovals highlight the same locations. In panel (b), the oval highlights the new narrow, linear depression, and the yellow arrows point to subtle traces of its extension.

Surfaces of sand can also provide rare constraints on quantitative age estimates of distinct depressions in ground patterns (as used in the preceding section). Sand itself, figures importantly in diverse ways in ground patterns and associated features. Sand-wedge growth, which drives the formation of the troughs with axial crack-like depressions very similar in appearance to those in Gale Crater, requires sustained addition of wind-blown sand. Moreover, sand surfaces can reveal small subsurface displacements in the form of surface cracks and offsets crossing active eolian ripples; these would be nearly imperceptible and easily missed on ordinary regolith surfaces that are less uniform. Lastly, sand highlights the patterns by lining the troughs, making them more visible as sand contrasts with the surrounding ground surface and bedrock outcrops (Figure 1).

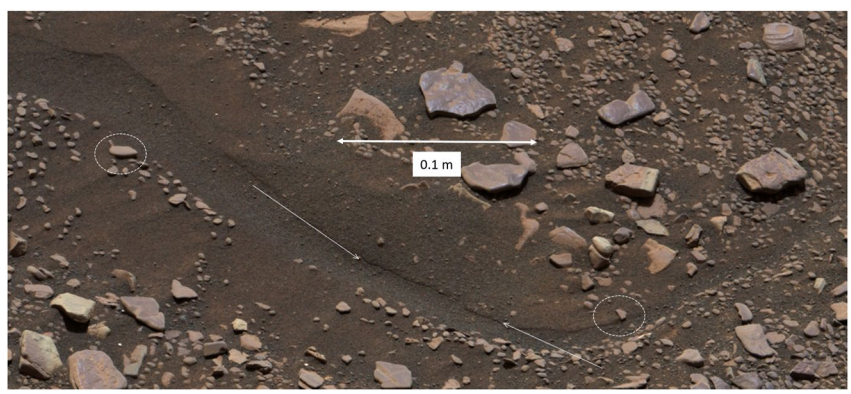

Figure 16. Surface details suggestive of recent activity along regolith troughs include delicate features that could not last long: a hairline crack in a trough at the base of a steep slope (marked with white arrows) and nearby teetering or overhanging stones (white circles). See Figure 5 for this image's location and broader context (Sol 2427, MR-012852).

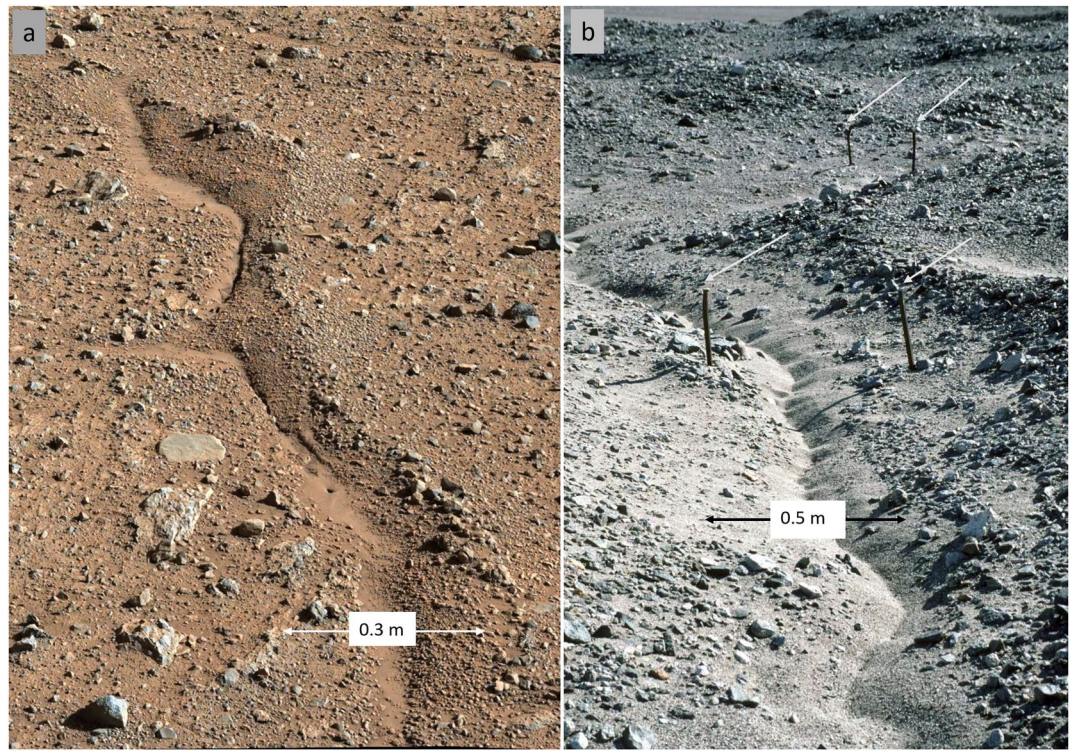

Figure 17. Distinct trench along the axis of a sandy trough bordered by stony ridges on Mars and Earth. (a) Mastcam image of a compound trough, encountered early in the Mars Science Laboratory mission on Sol 0590 (ML-002482). (b) Dry Valley site in Beacon Valley, Antarctica. The field of view straddles the edges of two adjacent sand-wedge polygons separated by an active trough that has been monitored for decades using vertical steel rods pounded into the frozen regolith (white arrows) (Black, 1976). Panel (b) courtesy of R. Sletten.

Before ending this subsection, we stress that considerations of expansion-contraction activity on Mars are not limited to the contemporary dry terrain in GT. Similar activity, but with much larger volumetric changes, is central to studies of many Martian paleo-settings with abundant water that subsequently desiccated, forming characteristic crack patterns. These range in scale and location from 10^{-2} m in the Murray formation, Gale Crater (Stein et al., 2018), to 10^{2} m in widespread locations on Mars (El-Maarry et al., 2014). Interestingly, El-Maarry et al. (2014) studied the global distribution of these larger patterns—potential desiccation polygons—and noted findings that relate directly to current and future research in Gale Crater and elsewhere on Mars. These polygons "are mostly associated with sedimentary deposits that display spectral evidence for the presence of Fe/Mg smectites, Al-rich smectites or less commonly sulfates… [They] may indicate paleolacustrine environments, which are of high interest for planetary exploration, and their presence implies that the fractured units are rich in smectite minerals that may have been deposited in a standing body of water."

5.4. Dual Drivers for Volumetric Cycling: Temperature and Humidity Variations

Polygonal patterned ground occurs on Earth where seasonal temperature variations are large and the ground is ice-rich. The dominant driver for the expansion-contraction activity is the varying surface temperature due to atmosphere-surface energy exchange. Ice provides cohesion to the regolith, permitting volumetric changes and resulting stresses to develop on scales comparable to the depth of penetration of environmental variations. Without ice or another source of cohesion, volumetric changes are limited to the size of individual particles. Furthermore, ice contributes directly to the expansion-contraction activity because of its relatively high coefficient of thermal expansion.

On Mars, near the equator, volumetric changes in the regolith and underlying bedrock likely arise from significant surface variations in humidity, as well as temperature (Figure 14). The relative importance of these environmental

drivers is not evident, however, because little is known about the thermo-mechanical and adsorption properties of the Gale bedrock and regolith; in particular, their effective coefficients of thermal expansion and coefficients of "hydric" expansion are unknown. The frequency of the diurnal variation in ground temperature is clearly too high to penetrate more than a few centimeters below the ground surface (Vasavada et al., 2017). Hence, although it is large, it does not readily account for ground patterns extending over meters or more. Deeper penetration implies lower frequency surface forcings, suggesting that seasonal variations in both temperature and humidity, which are significant (Figure 14), could help account for the observed ground patterns.

In Gale Crater, temperature-induced volumetric variations in the regolith and underlying bedrock are expected to be smaller than in terrestrial sand-wedge polygon areas because seasonal temperature changes are smaller than in polar regions on Earth, and the bedrock has a lower coefficient of thermal expansion than ice-rich permafrost. On the other hand, seasonal humidity variations are quite distinct at the base of the atmosphere in Gale Crater (Figure 14), and the dry bedrock just below the ground surface would likely respond readily to humidity variations, especially in the GT region where the bedrock is clay-rich.

5.5. Consequences of Expansion-Contraction Activity in Regolith and Bedrock

Much as shallow surface troughs form over sand-wedges on Earth (Pewe, 1959), similar troughs could form incrementally in thin regolith in Gale Crater where contraction of underlying bedrock blocks causes intervening bedrock gaps to widen. The gaps would partially fill with sand or small rock fragments when open and close when the bedrock expands. Cyclic opening and closing of these gaps, repeated over extended periods, together with the addition of wind-blown sand at the surface would lead to near-vertical, narrow wedges of sandy regolith that grow incrementally with time. The widening of wedges would effectively stretch the overlying regolith in the direction normal to the wedge, thereby providing a driver for the particle organization and sorting. It would also help account both for troughs forming over the wedges and for axial trenches developing along the troughs over shallow subsurface cracks. This scenario is consistent with field evidence, including the opening of the crack-like linear depression documented at Woodland Bay (Figures 6c and 15) and active downslope displacement of grains documented at Upper Ollach without filling the center of the axial trench (Figure 9, and animated GIF, Figure S4, in the Supporting Information). In this context, the crack-like linear depression that formed at Woodland Bay would naturally develop into an axial trench similar to those occurring nearby and in other sites.

Such incremental widening of bedrock gaps could continue essentially unimpeded for extended periods where bedrock blocks are surrounded by loose regolith. On the other hand, for domains comprised largely of bedrock, which is inherently less deformable than regolith, the gaps between adjacent bedrock blocks cannot widen indefinitely and sustain the infilling because of the mechanical constraints imposed by the surrounding bedrock. At least two factors and processes would, however, solve or alleviate the implicit space problem. First, the bedrock in GT is far from incompressible; it is rich in visible open spaces—pores, voids, and cracks—that could shrink and/or accommodate fine-grained mineral grains filtering down from the surface. The bedrock density for Gale is estimated to be 1,680 ± 180 kg m^{-3} (Lewis et al., 2019). Assuming the density of mineral grains, typical of a basaltic parent rock, is between 2,750 and 2,850 kg m^{-3}, this range of plausible bulk density values corresponds to bedrock void ratios between 32% and 47%. Second, venting of volatiles from depth could conceivably move fine buried material to the surface, as proposed by Horne (2018), to form "leveed fissures." However, as mentioned earlier, we know of no evidence for such venting in GT. Moreover, the source of the volatiles at depth is unknown and venting does not readily account for many of the pattern characteristics, including their shape, relief, sorting, and surface texture.

5.6. Factors Controlling the Expansion-Contraction Activity

Salts in the subsurface are expected to affect the inferred volumetric variations of the regolith and bedrock. Any adsorbed water in the regolith would be affected by salts. High solute contents would strongly decrease the chemical potential of water and lower its freezing point well below 0°C (Hillel, 1998). Low temperatures also slow adsorption kinetics and strongly reduce the liquid water content of sub-0°C regolith and rock (Vugmeyster et al., 2017); both effects impede the diffusion of water vapor through the subsurface (Bryson et al., 2008; Chevrier et al., 2006; Hanley et al., 2011; Liu et al., 2015). Salts with extremely low eutectic temperatures are present on Mars (Kounaves et al., 2010), and abundant chloride salts have been detected in Gale Crater (Thomas

et al., 2019). They have high degrees of hydration (Fernanders et al., 2022) and may be primary H_2O reservoirs in the hydro-active layer (Martín-Torres et al., 2015). In addition, hydrating salts would change vapor density gradients in dry soil, influencing the seasonal pattern of water vapor flux and the net flux to the atmosphere (Schorghofer & Aharonson, 2005). Other factors are also expected to affect the vapor transport in and out of the regolith, including porosity, particle size, and surface area.

An increase in humidity or a decrease in temperature induces hydration and surface adsorption. Under Earth conditions, laboratory studies of specimens of diverse rock types that are not water-saturated show that increasing air humidity generally causes significant swelling in shales (Huang et al., 1995), mudrocks (Venter, 1981), and even crystalline rocks (Schult & Shi, 1997). Venter (1981) studied a suite of diverse "mudrock" samples that may serve well as analogs to the mudstones in GT. Temperature changes reaching 45°C did not affect their volume significantly. However, even small changes in RH caused fluctuations in volume. "A maximum shrinkage of 0.34% took place with a drop in RH from 88% to 60%, and a maximum shrinkage of 0.49% took place with a drop in RH from 90% to 22%." The corresponding minimum shrinkage was less than 0.05%, illustrating the large shrinkage range for different mudstone samples. Regardless of which sample is most like the bedrock in GT, these data suggest that the RH-induced shrinkage on Earth is large relative to reasonable estimates of thermal contraction. For instance, the reported range of shrinkage (0.05%–0.5%) caused by a drop in RH from 90% to 22% is equivalent to contraction due to a cooling of 30°C–300°C, assuming a relatively high coefficient of thermal expansion representative of various clay minerals (15×10^{-6} °C^{-1}; McKinstry, 1965). While salts generally contribute to swelling via hydration, Schult and Shi (1997) reported a reduction of swelling after saturating soil samples with $CaCl_2$ solutions presumably, due to the neutralization of repulsive surface forces.

GT tends to have high smectite concentrations (Tu et al., 2021). This smectite is generally believed to have formed in the distant past; however, smectite formation in the salt-rich regolith may also be contemporary (Bish et al., 2003). A study at an analog site in the Dry Valleys of Antarctica recognized that smectite minerals have formed there recently and may be currently forming at temperatures as low as −21°C where salts in the permafrost significantly enhance weathering by increasing the unfrozen water (Cuozzo et al., 2020); they aptly named the region, in which liquid water is present seasonally at temperatures well below 0°C, the "eutectic active layer." Thermodynamic modeling using PHREEQ supports the field findings; it suggests that smectite may form at subzero temperatures in liquid brine films on mineral fragments in Antarctic permafrost. The formation of smectites in Mars permafrost would contribute to the regolith's expansion-contraction activity.

5.7. Roles of Lithology, Mineralogy, and Environmental Conditions in Glen Torridon

As mentioned above, ground patterns are not limited to the GT region or to bedrock areas rich in clays. In particular, the distinct sandy border around adjacent bedrock blocks at Rock Hall (Figure 4) raised much attention, and yet, at this location, clays account for only 13% of the minerals (e.g., Rampe et al., 2020). Hence, the patterns occur locally across the suite of diverse sedimentary bedrock terrain and different formations—the Murray and Carolyn Shoemaker formations—traversed in GT by Curiosity. Nevertheless, the abundance of smectite in the GT area (up to ∼30%, Thorpe et al., 2021) most likely accounts for ground patterns appearing unusually common and distinct in the area. Moreover, both the sites that we studied most extensively—Woodland Bay and Mary Anning—were in the lower portion of GT, where clay minerals (and red hematite) are ubiquitous (Rudolph et al., 2021). The bedrock mineralogy could contribute to the ground patterns either directly through the adsorption and mechanical properties of the bedrock that control volumetric changes or through the regolith's properties that are likely comprised mainly of weathered local bedrock. We note that the Dynamic Albedo of Neutrons measurements (Czarnecki et al., 2022) show unusually high water-equivalent hydrogen values, reaching 5%, at some sites with well-developed ground patterns.

The large variations in temperature and humidity measured in Gale Crater in the atmosphere near the ground surface are expected to cause significant cyclic expansion and contraction in the bedrock and regolith. In the context of the robust environmental trends monitored during the entire duration of the MSL mission (Figure 14), however, environmental variations were not unusual for Gale Crater during the period of Curiosity's traverse of GT (outlined in Figure 14). Derived surface properties, such as albedo and thermal inertia, were also not unusual (Martínez et al., 2021). Hence, measured environmental conditions and derived surface properties do not seem to account for the apparent relative abundance of ground patterns in GT.

The 61-sol period during which a crack-like depression formed in the Woodland Bay area (marked by the shading in Figure 14) is of special interest in this context. The simplest expectation would be for the depression to form while the adjacent bedrock contracted during a drying or cooling period. Figure 14 shows a clear cooling trend during this period, but the surface temperature drop is small (~5°C–6°C) and there is little variation in RH. However, as in other diffusional systems subjected to cyclic external forcing, volumetric variations below the ground surface would lag the surface forcing. The duration of this lag would increase with depth, but assessing it would be challenging due to the lack of information about the transport and mechanical properties of subsurface material and due to the presence of shallow voids and bedding-parallel discontinuities in the sedimentary bedrock that cause inhomogeneous and complex thermal coupling between the surface and subsurface material (e.g., Vasavada et al., 2017). These bedrock discontinuities are inferred from exposures and observations that rover wheels frequently dislodged rock slabs that appeared to be coherent bedrock.

Lastly, we stress that Figure 14 only shows single daily values for temperature and humidity because it was designed to highlight the seasonal and other long-period environmental variations. We focus on these because they seem more likely to drive volumetric variations well below the ground surface in the bedrock. Hence, Figure 14 does not show the large diurnal swings in temperature, with changes often approaching 100°C. And yet, in the context of recent work on granular creep (introduced at the end of Section 6), these high-frequency environmental variations could significantly accelerate the slow movement (creep) of loose surface sand and similar material on Mars. Moreover, surface disturbances by impacts of wind-driven saltating particles would likely have a similar accelerating effect on near-surface creep.

5.8. The Expansion-Contraction Activity: An Atmospheric Science Perspective

Interest in vapor exchange between the regolith and the atmosphere extends well beyond its role in the expansion-contraction activity in the regolith and ground patterns. It has long been recognized within the atmospheric science community and was extensively studied early in the MSL mission (Martín-Torres et al., 2015; Martínez et al., 2021; Savijärvi et al., 2015). According to Martin-Torres et al. (2015), the diurnal and seasonal variations of H_2O vmr (volumetric mixing ratio) in the atmosphere, as measured by REMS 1.6 m above the surface, suggest that water is absorbed and released by the regolith, presumably by adsorption and desorption on salts, clays, and other minerals, such as sulfates, that can contain and exchange significant amounts of water. They used the diurnal change variation of H_2O vmr to estimate the depth of the hydro-active layer (an alternate term for the eutectic active layer introduced earlier); for regolith with about 0.1 wt% of Ca-perchlorate, it is a few centimeters. It is worth noting that while daily changes may not penetrate enough to cause significant volumetric changes at depth, seasonal climate variations (e.g., Figure 14) could lead to substantial changes in the regolith and bedrock to depths approaching or exceeding meters, the typical size of the ground patterns, and by inference, the depth to which significant granular organization extends below the surface.

Martin-Torres et al. (2015) also inferred broad implications for the hydro-active layer. They ranged from atmospheric modeling and remote sensing interpretation and involved a spectrum of planet-wide properties and activities, including the oxidation state of the upper crust, the global water cycle, future exploration, and habitats on Mars.

5.9. Role of Rover Disturbances

The potential role of rover-induced disturbances in the observations reported herein is complex because of the diversity of terrain properties (roughness, bedrock, and regolith distribution at, and directly below, the ground surface) and the variety of rover activities; they are beyond the scope of this paper, but the role of obvious disturbances is summarized. The primary disturbance to the terrain arises from the impact of moving rover wheels, vibrations caused by drilling, and—to a much smaller extent—other rover activities (e.g., camera or robotic arm motion). Significant visible rover disturbances of the ground are clearly localized under and near the wheels, seldom extending beyond tens of millimeters from the wheels. At Mary Anning, however, ground vibrations caused by the drilling of three bedrock holes caused considerable surface change within nearly 1 m of the drilling site, with distinct displacements of loose rock fragments and granules, formation of trough-parallel scarps and fissures, and subsidence with local collapsed areas along the center of an axial trench (Sol 2840 inset in Figure 9; see Figures S3 and S4, an animated GIF, in Supporting Information).

On the other hand, disturbances were unusually small in several sites of special interest, including Woodland Bay, where there was no drilling, and where Curiosity did not rove over the ground pattern; in addition, it traveled ~100 m away before returning 61 sols later. The rover left no visible impact on the micro-topography and granular organization of this pattern (Figures 5 and 6). It may, however, have provided the trigger for local subsidence, such as manifested in the new narrow, linear surface depression that formed within the 61-sol period (Figure 15). This subsidence requires a preexisting subsurface void structure along the axis of a broad sandy trough, much like that which develops between sand wedge polygons on Earth after a multitude of expansion-contraction cycles. The trace of surface subsidence probably reflects the descent of small rocks and sand from the subsurface into subsurface voids and from collapse of the void structure. The subsidence most likely would have occurred without rover disturbance, but the rover may have impacted its timing. Sand or fine-grained regolith sifting down into a near-vertical gap between shallow bedrock blocks would naturally form a narrow depression along the inferred joints, thereby accounting for the alignment and position of the fresh narrow, linear surface depression.

The impact of the extensive drilling was large and disruptive, but it also yielded significant collateral benefits: (a) information about the mechanical coupling of the drilled bedrock surface to the subsurface, (b) an opportunity to study the regolith surface response to large perturbations, the timing of which is precisely known, and (c) an exceptionally long observation period. Significant grain motion reaching 1–2 cm was evident on relatively stable sand surfaces (well below the angle of repose) during periods extending as long as 10 to 15 sols after the drilling stopped. In addition, the disturbances seem to cause the central portions of the trough, Upper Ollach, to subside and locally collapse, steepening the side slopes of the trough and accelerating downslope grain motion (Figure 9; Figures S3 and S4, an animated GIF). In essence, this mimicked, in extreme fast motion, the inferred effects of natural volumetric cycling that cause granular organization between near-surface bedrock blocks, subsidence along the center of the troughs, and formation of the axial trenches discussed above.

6. Potential Geomorphic Implications of Expansion-Contraction Activity

We speculate that cyclic expansion-contraction activity not only drives the formation of ground patterns but has broad implications for landscape evolution on Mars through at least three universal geomorphic processes: (a) mechanical weathering, (b) chemical weathering, and (c) downslope creep.

1. The fracture of bedrock, as well as the generation and comminution of rock debris, to form regolith on Mars could partly be due to expansion-contraction activity in the shallow subsurface. For instance, large local stresses are expected to arise recurrently in coarse debris surrounded by bedrock when it expands due to rising temperature or humidity. This activity may contribute to the common occurrence of large rock fragments at the edges of extensive bedrock exposure and their tilting toward vertical (see Section 5.3). The lateral expansion of bedrock domains, due to increasing atmospheric temperature or humidity, is expected to scale with the size of the domain. Hence regolith adjacent to larger bedrock domains would be subjected to relatively large boundary displacements. This would, in turn, generate elevated contact stresses along the bedrock-regolith interface as well as enhanced comminution and granular organization of the regolith adjacent to extensive bedrock domains, perhaps helping account for the preferential distribution of rock fragments surrounding major bedrock structures (Figure 12). The contact stresses originating from the inferred large-scale expansion-contraction activity in the regolith and bedrock would add to the local internal stresses, as well as thermal stresses in individual surface rocks directly due to recurrent solar exposure.
2. The second geomorphic process, chemical weathering, includes the formation of clay minerals. The generally enhancing effects of salts and clays on moisture exchange between the subsurface and the atmosphere, and by inference, on volumetric cycling in the bedrock, may provide positive feedback to a weathering loop, with the volumetric cycling accelerating mechanical weathering and the creation of fresh mineral surfaces, in turn enhancing chemical weathering and clay formation (see Section 5.6).
3. Lastly, expansion-contraction activity on rocky hillslopes would continuously disturb the regolith and adjacent bedrock, permitting regolith creep due to incremental grain rearrangements biased by gravity with grains ranging in size from sand to large bedrock blocks even on relatively gentle hillslopes with inclinations well below the angle of repose. On the small scale of eolian ripples and surface offsets, the cyclic environmental changes would affect sand surfaces by helping sustain microscopic granular displacements. This suggestion stems from novel experimental studies of the physics of sand piles that are casting brand new light on this seemingly familiar phenomenon. Deshpande et al. (2021) reported that "Surprisingly, we find that even an

undisturbed sandpile creeps indefinitely, with rates and styles comparable to natural hillslopes. Creep progressively slows as the initially fragile pile relaxes into a lower energy state. This slowing (dubbed 'aging') can be enhanced or reversed." They suggest a new "creeping glass" model … "wherein environmental disturbances maintain soil in a perpetually fragile state." Interestingly, these disturbances include thermal variations and variations in humidity (Bocquet et al., 2002) that are small compared to those measured with diurnal regularity on Mars. They would also include mechanical disturbances such as the expansion-contraction activity in the adjacent or underlying bedrock discussed through much of this paper and impacts ranging from saltating sand grains to meteors as well as seismic activity on Mars (Sun & Tkalčić, 2022). Hence, this new "creeping glass" model bears on diverse surface processes on Mars, including downslope creep, and the micro-relief evolution of eolian bedforms and regolith surfaces. Regarding the bedforms, the influence of the large diurnal temperature fluctuations on Mars warrants close attention in light of the recent finding that "a few seconds of heating was able to reverse 10^4 s of aging" (Deshpande et al., 2021) even for temperature changes much smaller than those occurring daily on Mars.

7. Conclusions

Images from the MSL rover, Curiosity, reveal distinct natural patterns on the ground near the equator on Mars, in the GT region of Gale Crater. These patterns contrast sharply with the typical, seemingly random scatter of rocks on smooth sandy ground surfaces and bedrock outcrops. The fresh appearance of the patterns and the documented surface changes during the observation period suggest that they are active on a timescale of tens of days to decades. The patterns are intrinsically interesting as remarkable examples of granular self-organization, a well-known phenomenon in diverse granular systems on Earth, but only recently revealed in detail on Mars by images from rovers.

The ground patterns share similarities with patterned ground in permafrost areas at high latitudes on both Earth and Mars but differ in lacking the regularity and widespread nature of patterned ground. Moreover, whereas typical patterned ground on Earth is best developed in deep regolith away from bedrock areas, GT patterns are only found adjacent to, or within 1–2 m of, bedrock exposures. A parsimonious explanation is that ground troughs bordering bedrock develop there because the regolith is thin enough that cyclic contraction of bedrock blocks recurrently opens intervening voids and cracks, allowing loose sand or other fine rock debris to filter down below the surface. Upon warming or increasing humidity, the voids and cracks would narrow but could not close completely. In the long term, a multitude of inferred expansion-contraction cycles, driven by the large environmental fluctuations in temperature and humidity, would incrementally form troughs in thin, dry regolith, each centered over a wedge of sand and small rocks, much as occurs in active sand-wedge polygons on Earth. The GT patterns are likely forms of self-organization in dry granular media, driven by oscillating transfers of energy and mass (i.e., H_2O) between the atmosphere and the terrain. These transfers may have significant implications for studies of contemporary near-surface atmospheric and geomorphic processes on Mars. Importantly, ground patterns should be interpreted with care; they do not signal current bulk water or ice near the equator of Mars.

These ground features are widespread but local and relatively infrequent along Curiosity's traverse. Because Curiosity has encountered distinct ground patterns only in a few sites within the small (<1 km^2) area of GT, over which environmental conditions are likely relatively uniform spatially, the scattered locations of the features must reflect unusual local subsurface properties or conditions that, though they may elude direct observation, are particularly favorable for the self-organization of regolith and pattern development. Hence, ground patterns may signal where the hydro-active layer is unusually active, possibly because the subsurface H_2O content is unusually high or close to the surface.

The ending of the preceding paragraph partly addresses the question raised in the introduction: What are the patterns "trying to tell us" about the conditions and processes under the Mars surface, which remain understudied and essentially unknown. Much like Horne (2018), we suggest that "hitherto-unrecognized surface processes" are currently active or young, and we tighten the meaning of "young" considerably. We reach quite different interpretations, however, of the rover observations. Based on images from MER, the Mars Exploration Rover Opportunity in the Meridiani Planum region, Horne (2018) interprets the surface features as signatures of liquid and gas emissions. In GT, we have not seen such signatures; instead, our observations suggest that the ground patterns arise progressively over extended periods from inferred volumetric cycling of near-surface bedrock, driven by environmental variations.

Data Availability Statement

NASA Mars rover camera images used for this study are openly available in the NASA Planetary Data System (PDS; https://pds.nasa.gov/). The REMS data are publicly available from the PDS Atmospheres Node (REMS: Mars Science Laboratory Rover Environmental Monitoring Station RDR Data V1.0, MSL-M-REMS-4-ENVEDR-V1.0, https://atmos.nmsu.edu/PDS/data/mslrem_1001. All raw images used in this paper can be found online at https://mars.nasa.gov/msl/multimedia/raw-images). Filters are provided to select particular dates and/or periods (MSL sol numbers) and cameras (M100 and M34).

Acknowledgments
The authors are grateful for NASA's support of the Mars Science Laboratory (MSL) mission and for the efforts of the large team of talented and dedicated scientists and engineers who made this work possible. The authors thank, in particular, Jason Van Beek and Tex Kubacki for their astute observations and, together with their Malin Space Science Systems colleagues, for their critical roles in acquiring the images. The authors also thank Michelle Minitti, Tim Olson, and Ken Edgett for their observations and help in obtaining instructive images. The authors appreciate insightful discussions with Doug Jerolmack, Nakul Deshpande, Lucas Goehring, Lu Liu, Quan-Xing Liu, Zhenpeng Ge, Allan Treiman, and Kevin Lewis, which benefitted this paper. The authors thank J. Levy and an anonymous reviewer for their careful evaluations and detailed comments that substantially improved the manuscript. A. G. Fairén was supported by the ERC-CoG #818602. M.-P. Zorzano has been partially funded by the Spanish State Research Agency (AEI) Project No. MDM-2017-0737 Unidad de Excelencia "María de Maeztu"-Centro de Astrobiología (INTA-CSIC) and by the Spanish Ministry of Science and Innovation (PID2019-104205GB-C21). Last but not least, B. Hallet and R. S. Sletten gratefully acknowledge sustained funding for their work through the MSL mission in a NASA grant awarded to MSSS.

References

Aranson, I., & Tsimring, L. (2008). *Granular patterns* (p. 307). Oxford University Press.
Bagnold, R. A. (1941). *The physics of blown sand and desert dunes* (p. 265). Methuen.
Baker, M. M., Lapotre, M. G., Minitti, M. E., Newman, C. E., Sullivan, R., Weitz, C. M., et al. (2018). The Bagnold Dunes in southern summer: Active sediment transport on Mars observed by the Curiosity rover. *Geophysical Research Letters*, *45*(17), 8853–8863. https://doi.org/10.1029/2018gl079040
Baker, M. M., Newman, C. E., Lapotre, M. A., Sullivan, R., Bridges, N. T., & Lewis, K. W. (2018). Coarse sediment transport in the modern Martian environment. *Journal of Geophysical Research: Planets*, *123*(6), 1380–1394. https://doi.org/10.1002/2017je005513
Bell, J. F., III, Godber, A., McNair, S., Caplinger, M., Maki, J., Lemmon, M., et al. (2017). The Mars Science Laboratory Curiosity rover Mastcam instruments: Preflight and in-flight calibration, validation, and data archiving. *Earth and Space Science*, *4*(7), 396–452. https://doi.org/10.1002/2016ea000219
Bennett, K. A., Fox, V. K., Bryk, A., Dietrich, W., Fedo, L. Edgar, M. T., et al. (2022). The Curiosity Rover's Exploration of Glen Torridon, Gale crater, Mars: An Overview of the Campaign and Scientific Results. *Journal of Geophysical Research: Planets*, e2022JE007185. https://doi.org/10.1029/2022JE007185
Berg, T. E., & Black, R. F. (1966). Preliminary measurements of growth of nonsorted polygons, Victoria Land, Antarctica. In J. C. F. Tedrow (Ed.), *Antarctic soils and soil forming processes* (pp. 62–108). America Geophysical Union.
Bish, D. L., William Carey, J., Vaniman, D. T., & Chipera, S. J. (2003). Stability of hydrous minerals on the Martian surface. *Icarus*, *164*(1), 96–103. https://doi.org/10.1016/s0019-1035(03)00140-4
Bishop, J., Yeşilbaş, M., Hinman, N., Burton, Z., Englert, P., Toner, J., et al. (2021). Martian subsurface cryosalt expansion and collapse as trigger for landslides. *Science Advances*, *7*(6), eabe4459. https://doi.org/10.1126/sciadv.abe4459
Black, R. F. (1973). Growth of patterned ground in Victoria Land, Antarctica. *Paper presented at permafrost: The North American Contribution to the 2nd International Conference*. National Academy of Sciences.
Black, R. F. (1976). Periglacial features indicative of permafrost: Ice and soil wedges. *Quaternary Research*, *6*(1), 3–26. https://doi.org/10.1016/0033-5894(76)90037-5
Bocquet, L., Charlaix, E., & Restagno, F. (2002). Physics of humid granular media. *Comptes Rendus Physique*, *3*(2), 207–215. https://doi.org/10.1016/s1631-0705(02)01312-9
Bridges, N. T., Geissler, P. E., McEwen, A. S., Thomson, B., Chuang, F. C., Herkenhoff, K. E., et al. (2007). Windy Mars: A dynamic planet as seen by the HiRISE camera. *Geophysical Research Letters*, *34*(23). https://doi.org/10.1029/2007gl031445
Bryson, K. L., Chevrier, V., Sears, D. W., & Ulrich, R. (2008). Stability of ice on Mars and the water vapor diurnal cycle: Experimental study of the sublimation of ice through a fine-grained basaltic regolith. *Icarus*, *196*(2), 446–458. https://doi.org/10.1016/j.icarus.2008.02.011
Chevrier, V., Mathé, P. E., Rochette, P., & Gunnlaugsson, H. P. (2006). Magnetic study of an Antarctic weathering profile on basalt: Implications for recent weathering on Mars. *Earth and Planetary Science Letters*, *244*(3), 501–514. https://doi.org/10.1016/j.epsl.2006.02.033
Chevrier, V. F., & Rivera-Valentin, E. G. (2014). Regolith-atmosphere water vapor transfer on Mars: Comparison between Phoenix TECP and MSL REMS data. *Paper presented at Eighth International Conference on Mars, Pasadena, CA*.
Cuozzo, N., Sletten, R. S., Hu, Y., Liu, L., Teng, F.-Z., & Hagedorn, B. (2020). Silicate weathering in Antarctic ice-rich permafrost: Insights using magnesium isotopes. *Geochimica et Cosmochimica Acta*, *278*, 244–260. https://doi.org/10.1016/j.gca.2019.07.031
Czarnecki, S., Hardgrove, C., Arvidson, R. E., Hughes, M. N., Schmidt, M. E., Henley, T. et al. (2022). Hydration of a Clay-Rich Unit on Mars, Comparison of Orbital Spectral Data to Rover Neutron Results. Paper presented at Lunar and Planetary Science Conference.
Deshpande, N. S., Furbish, D. J., Arratia, P. E., & Jerolmack, D. J. (2021). The perpetual fragility of creeping hillslopes. *Nature Communications*, *12*(1), 3909. https://doi.org/10.1038/s41467-021-23979-z
Edgett, K. S., Yingst, R. A., Ravine, M. A., Caplinger, M. A., Maki, J. N., Ghaemi, F. T., et al. (2012). Curiosity's Mars Hand Lens Imager (MAHLI) investigation. *Space Science Reviews*, *170*(1), 259–317. https://doi.org/10.1007/s11214-012-9910-4
El-Maarry, M. R., Watters, W., McKeown, N. K., Carter, J., Noe Dobrea, E., Bishop, J. L., et al. (2014). Potential desiccation cracks on Mars: A synthesis from modeling, analogue-field studies, and global observations. *Icarus*, *241*, 248–268. https://doi.org/10.1016/j.icarus.2014.06.033
Fedo, C. M., Bryk, A. B., Edgar, L. A., Bennett, K. A., Fox, V. K., Dietrich, W. E., et al. (2022). Geology and stratigraphic correlation of the Murray and Carolyn shoemaker formations across the Glen Torridon region, Gale Crater, Mars. *Journal of Geophysics: Planets*, *127*, e2022JE007408. https://doi.org/10.1029/2022JE007408
Fernanders, M. S., Gough, R. V., Chevrier, V. F., Schiffman, Z. R., Ushijima, S. B., Martinez, G. M., et al. (2022). Water uptake by chlorate salts under Mars-relevant conditions. *Icarus*, *371*, 114715. https://doi.org/10.1016/j.icarus.2021.114715
Gajjar, P., Johnson, C. G., Carr, J., Chrispeels, K., Gray, J. M. N. T., & Withers, P. J. (2021). Size segregation of irregular granular materials captured by time-resolved 3D imaging. *Scientific Reports*, *11*(1), 8352. https://doi.org/10.1038/s41598-021-87280-1
Hallet, B., Sletten, R., & Whilden, K. (2011). Micro-relief development in polygonal patterned ground in the Dry Valleys of Antarctica. *Quaternary Research*, *75*(2), 347–355. https://doi.org/10.1016/j.yqres.2010.12.009
Hanley, J., Rivera-Valentin, E., & Chevrier, V. (2011). Control of the water cycle by the regolith at the Phoenix landing site. *Mars Atmosphere: Modelling and observation*, 247–250.
Hillel, D. (1998). *Environmental soil physics*. Academic Press.
Horne, D. J. (2018). Young, small-scale surface features in Meridiani Planum, Mars: A possible signature of recent transient liquid and gas emissions. *Planetary and Space Science*, *157*, 10–21. https://doi.org/10.1016/j.pss.2018.04.012

Huang, S. L., Speck, R. C., & Wang, Z. (1995). The temperature effect on swelling of shales under cyclic wetting and drying. *International Journal of Rock Mechanics and Mining Sciences & Geomechanics Abstracts*, *32*(3), 227–236. https://doi.org/10.1016/0148-9062(94)00044-4

Kostama, V. P., Kreslavsky, M., & Head, J. (2006). Recent high-latitude icy mantle in the northern plains of Mars: Characteristics and ages of emplacement. *Geophysical Research Letters*, *33*(11), 2006GL025946. https://doi.org/10.1029/2006gl025946

Kounaves, S. P., Hecht, M. H., Kapit, J., Gospodinova, K., DeFlores, L., Quinn, R. C., et al. (2010). Wet chemistry experiments on the 2007 Phoenix Mars Scout Lander mission: Data analysis and results. *Journal of Geophysical Research*, *115*(E1), 1–16. https://doi.org/10.1029/2009JE003424

Kuzmin, R. O. (2005). 7 Ground ice in the Martian regolith. In T. Tokano (Ed.), *Water on mars and life* (pp. 155–189). Springer.

Lachenbruch, A. H. (1962). *Mechanics of thermal contraction cracks and ice-wedge polygons in permafrost* (p. 69). Geological Society of America.

Laskar, J., Correia, A., Gastineau, M., Joutel, F., Levrard, B., & Robutel, P. (2004). Long term evolution and chaotic diffusion of the insolation quantities of Mars. *Icarus*, *170*(2), 343–364. https://doi.org/10.1016/j.icarus.2004.04.005

Levy, J., Head, J., & Marchant, D. (2009). Thermal contraction crack polygons on Mars: Classification, distribution, and climate implications from HiRISE observations. *Journal of Geophysical Research*, *114*(E1), E01007. https://doi.org/10.1029/2008je003273

Lewis, K. W., Peters, S., Gonter, K., Morrison, S., Schmerr, N., Vasavada, A. R., & Gabriel, T. (2019). A surface gravity traverse on Mars indicates low bedrock density at Gale Crater. *Science*, *363*(6426), 535–537. https://doi.org/10.1126/science.aat0738

Liu, L., Sletten, R. S., Hagedorn, B., Hallet, B., McKay, C. P., & Stone, J. O. (2015). An enhanced model of the contemporary and long-term (200 ka) sublimation of the massive subsurface ice in Beacon Valley, Antarctica. *Journal of Geophysical Research: Earth Surface*, *120*(8), 1596–1610. https://doi.org/10.1002/2014JF003415

Madeleine, J.-B., Forget, F., Head, J. W., Levrard, B., Montmessin, F., & Millour, E. (2009). Amazonian northern mid-latitude glaciation on Mars: A proposed climate scenario. *Icarus*, *203*(2), 390–405. https://doi.org/10.1016/j.icarus.2009.04.037

Malin, M. C., Ravine, M. A., Caplinger, M. A., Tony Ghaemi, F., Schaffner, J. A., Maki, J. N., et al. (2017). The Mars Science Laboratory (MSL) Mast cameras and descent imager: Investigation and instrument descriptions. *Earth and Space Science*, *4*(8), 506–539. https://doi.org/10.1002/2016EA000252

Mangold, N. (2005). High latitude patterned grounds on Mars: Classification, distribution and climatic control. *Icarus*, *174*(2), 336–359. https://doi.org/10.1016/j.icarus.2004.07.030

Martínez, G., Vicente-Retortillo, A., Vasavada, A., Newman, C., Fischer, E., Rennó, N., et al. (2021). The surface energy budget at Gale Crater during the first 2500 sols of the Mars Science Laboratory mission. *Journal of Geophysical Research: Planets*, *126*(9), e2020JE006804. https://doi.org/10.1029/2020je006804

Martín-Torres, F. J., Zorzano, M.-P., Valentín-Serrano, P., Harri, A.-M., Genzer, M., Kemppinen, O., et al. (2015). Transient liquid water and water activity at Gale Crater on Mars. *Nature Geoscience*, *8*(5), 357–361. https://doi.org/10.1038/ngeo2412

McKinstry, H. A. (1965). Thermal expansion of clay minerals. *American Mineralogist: Journal of Earth and Planetary Materials*, *50*(1–2), 212–222.

Mellon, M. T., Arvidson, R. E., Marlow, J. J., Phillips, R. J., & Asphaug, E. (2008). Periglacial landforms at the Phoenix landing site and the northern plains of Mars. *Journal of Geophysical Research*, *113*, E00A23. https://doi.org/10.1029/2007je003039

Mellon, M. T., Arvidson, R. E., Sizemore, H. G., Searls, M. L., Blaney, D. L., Cull, S., et al. (2009). Ground ice at the Phoenix landing site: Stability state and origin. *Journal of Geophysical Research*, *114*(E1), E00E07. https://doi.org/10.1029/2009je003417

Mellon, M. T., & Sizemore, H. G. (2022). The history of ground ice at Jezero Crater Mars and other past, present, and future landing sites. *Icarus*, *371*, 114667. https://doi.org/10.1016/j.icarus.2021.114667

Mitrofanov, I., Malakhov, A., Djachkova, M., Golovin, D., Litvak, M., Mokrousov, M., et al. (2022). The evidence for unusually high hydrogen abundances in the central part of Valles Marineris on Mars. *Icarus*, *374*, 114805. https://doi.org/10.1016/j.icarus.2021.114805

Mutch, T. A., Arvidson, R. E., Binder, A. B., Guinness, E. A., & Morris, E. C. (1977). The geology of the Viking Lander 2 site. *Journal of Geophysical Research*, *82*(28), 4452–4467. https://doi.org/10.1029/JS082i028p04452

Mutch, T. A., Grenander, S. U., Jones, K. L., Patterson, W., Arvidson, R. E., Guinness, E. A., et al. (1976). The surface of Mars: The view from the Viking 2 lander. *Science*, *194*(4271), 1277–1283. https://doi.org/10.1126/science.194.4271.1277

Newman, C. E., Gómez-Elvira, J., Marin, M., Navarro, S., Torres, J., Richardson, M. I., et al. (2017). Winds measured by the Rover Environmental Monitoring Station (REMS) during the Mars Science Laboratory (MSL) rover's Bagnold Dunes Campaign and comparison with numerical modeling using MarsWRF. *Icarus*, *291*, 203–231. https://doi.org/10.1016/j.icarus.2016.12.016

Oehler, D. Z., Mangold, N., Hallet, B., Fairén, A. G., Deit, L. L., Williams, A. J., et al. (2016). Origin and significance of decameter-scale polygons in the lower Peace Vallis fan of Gale Crater, Mars. *Icarus*, *277*, 56–72. https://doi.org/10.1016/j.icarus.2016.04.038

Pelletier, J. D., Leier, A. L., & Steidtmann, J. R. (2009). Wind-driven reorganization of coarse clasts on the surface of Mars. *Geology*, *37*(1), 55–58. https://doi.org/10.1130/g25071a.1

Pewe, T. L. (1959). Sand-wedge polygons (tesselations) in the McMurdo Sound region, Antarctica; a progress report. *American Journal of Science*, *257*(8), 545–552. https://doi.org/10.2475/ajs.257.8.545

Rampe, E. B., Blake, D. F., Bristow, T. F., Ming, D. W., Vaniman, D. T., Morris, R. V., et al. (2020). Mineralogy and geochemistry of sedimentary rocks and eolian sediments in Gale Crater, Mars: A review after six Earth years of exploration with curiosity. *Geochemistry*, *80*(2), 125605. https://doi.org/10.1016/j.chemer.2020.125605

Rosato, A. D., & Windows-Yule, C. (2020). *Segregation in vibrated granular systems*. Academic Press.

Rudolph, A., Horgan, B., Johnson, J., Bennett, K., Haber, J., Fox, V., et al. (2021), Diagenesis in the Glen Torridon Region of Gale Crater, Mars UsingVNIR Spectral Data from Curiosity Rover. Paper presented at Lunar and PlanetaryScience Conference.

Savijärvi, H. I., Harri, A.-M., & Kemppinen, O. (2015). Mars Science Laboratory diurnal moisture observations and column simulations. *Journal of Geophysical Research: Planets*, *120*(5), 1011–1021. https://doi.org/10.1002/2014JE004732

Schmidt, F., Andrieu, F., Costard, F., Kocifaj, M., & Meresescu, A. G. (2017). Formation of recurring slope lineae on Mars by rarefied gas-triggered granular flows. *Nature Geoscience*, *10*(4), 270–273. https://doi.org/10.1038/ngeo2917

Schorghofer, N., & Aharonson, O. (2005). Stability and exchange of subsurface ice on Mars. *Journal of Geophysical Research*, *110*(E5), E05003. https://doi.org/10.1029/2004je002350

Schult, A., & Shi, G. (1997). Hydration swelling of crystalline rocks. *Geophysical Journal International*, *131*(1), 179–186. https://doi.org/10.1111/j.1365-246x.1997.tb00604.x

Sletten, R., Hallet, B., & Fletcher, R. (2003). Resurfacing time of terrestrial surfaces by the formation and maturation of polygonal patterned ground. *Journal of Geophysical Research*, *108*(E4), 8044. https://doi.org/10.1029/2002JE001914

Stein, N., Grotzinger, J., Schieber, J., Mangold, N., Hallet, B., Newsom, H., et al. (2018). Desiccation cracks provide evidence of lake drying on Mars, Sutton Island member, Murray formation, Gale Crater. *Geology*, *46*(6), 515–518. https://doi.org/10.1130/g40005.1

Sullivan, R., Baker, M., Newman, C., Turner, M., Schieber, J., Weitz, C. et al. (2022) The Aeolian Environment in Glen Torridon, Gale crater, Mars. *Journal of Geophysical Research: Planets*, e2021JE007174. https://doi.org/10.1029/2021JE007174

Sun, W., & Tkalčić, H. (2022). Repetitive marsquakes in Martian upper mantle. *Nature Communications*, *13*(1), 1–9. https://doi.org/10.1038/s41467-022-29329-x

Thomas, N. H., Ehlmann, B. L., Meslin, P.-Y., Rapin, W., Anderson, D. E., Rivera-Hernández, F., et al. (2019). Mars Science Laboratory observations of chloride salts in Gale Crater, Mars. *Geophysical Research Letters*, *46*(19), 10754–10763. https://doi.org/10.1029/2019GL082764

Thorpe, M., Bristow, T., Rampe, E., Grotzinger, J., Fox, V., Bennett, K., et al. (2021). The mineralogy and sedimentary history of the Glen Torridon region, Gale Crater, Mars. *Paper presented at Lunar and Planetary Science Conference*.

Tu, V. M., Rampe, E. B., Bristow, T. F., Thorpe, M. T., Clark, J. V., Castle, N., et al. (2021). A review of the phyllosilicates in Gale Crater as detected by the CheMin instrument on the Mars Science Laboratory, Curiosity rover. *Minerals*, *11*(8), 847. https://doi.org/10.3390/min11080847

Vakkada Ramachandran, A., Zorzano, M.-P., & Martín-Torres, J. (2021). Experimental investigation of the atmosphere-regolith water cycle on present-day Mars. *Sensors*, *21*(21), 7421. https://doi.org/10.3390/s21217421

Vasavada, A. R., Piqueux, S., Lewis, K. W., Lemmon, M. T., & Smith, M. D. (2017). Thermophysical properties along Curiosity's traverse in Gale Crater, Mars, derived from the REMS ground temperature sensor. *Icarus*, *284*, 372–386. https://doi.org/10.1016/j.icarus.2016.11.035

Venter, J. P. (1981). The behaviour of some South African mudrocks due to temperature and humidity changes with particular reference to moisture content and volume changes. *The Proceedings of the International Symposium on Weak Rock*. International Society for Rock Mechanics.

Vugmeyster, L., Hagedorn, B., Clark, M. A., & Sletten, R. S. (2017). Evaluating the effect of grain size and salts on liquid water content in frozen soils of Antarctica by combining NMR, chemical equilibrium modeling, and scattered diffraction analysis. *Geoderma*, *299*, 25–31. https://doi.org/10.1016/j.geoderma.2017.03.024

Wang, A., Ling, Z., Yan, Y., McEwen, A. S., Mellon, M. T., Smith, M. D., et al. (2019). Subsurface Cl-bearing salts as potential contributors to recurring slope lineae (RSL) on Mars. *Icarus*, *333*, 464–480. https://doi.org/10.1016/j.icarus.2019.06.024